AD 678149

[redacted]

Distribution of this document is unlimited.

GENERAL DYNAMICS

ASTRONAUTICS

NOV 27 1968

A2136-1 (REV. 6-61)

REPORT NO. AE61-1140

DATE 7 Nov. 1961

NO. OF PAGES

AD 678149

CONVAIR ASTRONAUTICS

CONVAIR DIVISION OF GENERAL DYNAMICS CORPORATION

ACOUSTIC EVALUATION OF A WATER-COOLED FLAME BUCKET

Distribution of this document is unlimited.

PREPARED BY A. L. Shulman

CHECKED BY G. C. Wilson

CHECKED BY J. C. Ballinger

APPROVED BY W. H. Mitchell
Chief of Aerophysics

APPROVED BY W. F. Radcliffe
Chief Development Engineer

REVISIONS

NO.	DATE	BY	CHANGE	PAGES AFFECTED

FORM NO. A-700-1

AE61-1140
7 November 1961

FOREWORD

The purpose of this test was two fold. An acoustic evaluation of a water-cooled flame bucket was desired so that both near and far field noise reduction effects could be determined. An effort was made to simulate water flow conditions that would result from gravity flow from a large reservoir over a set of four weirs.

Test results are presented in graphical form for microphones located in both near and far field locations. Analysis of the data indicates an optimum water flow rate to exist for various locations in the acoustic field. An attempt is made to explain the phenomenon in terms of theoretical relationships and properties of the fluid flow. Suggestions are made for further analysis of these test results as well as future studies. Several modifications are proposed for the present test equipment.

TABLE OF CONTENTS

LIST OF ILLUSTRATIONS

LIST OF ILLUSTRATIONS (CONT.)

AE61-1140
7 Nov. 1961

SUMMARY

A series of small-scale model rocket tests was performed to evaluate the acoustical performance of water-cooled flame buckets. Data collected from these tests indicated the change in sound pressure level is a function of water flow-rate ratios for locations in both the near and far field. The water flow-rate ratio is defined as: water flow rate/propellant flow rate. Reductions of up to 12 db in the noise level were observed in the 1200-2400 cps band for conditions in the far field with a water flow-rate ratio of 3.33/1. This octave band converts to a Strouhal number of 0.045, which lies within the peak of generalized data from previously reported tests. The Strouhal number = $f_m \frac{d}{U}$, where f_m is the mean geometric frequency of a particular octave band, d is the rocket exit diameter in feet, and U the rocket exhaust mean velocity in feet/second.

AE61-1140
7 Nov. 1961

INTRODUCTION

The proposed series of large booster rockets now under consideration for space exploration presents serious problems for the static testing of rocket engines. The difficulty of transporting these large engines from the place of manufacture will require that static test sites be built close to large centers of population. The acoustic environment of such a situation would be intolerable if measures were not taken to modify the test site. These modifications should result in a change in directivity of the acoustic field and a reduction in the acoustic power at the source.

The present test was intended to be exploratory in nature and to indicate whether the direct injection of water into a flame bucket would be an efficient and practical means of noise reduction.

DESCRIPTION OF TEST PROGRAM

The model rocket engines used in this test had an exit diameter of 1.5 inches. The weight flow of propellants per engine was 0.75 pounds per second, and the jet stream power was approximately 3.4×10^5 watts (Reference 1). Two engine operation was used at all times during the test.

The flame bucket was designed and developed by the Thermodynamics Laboratory of General Dynamics/Convair (Reference 2). A sketch of the flame bucket is shown in Figure 1. The water injection system was designed to simulate gravity flow over a set of four weirs. Figure 2 shows an overall view of the test site during a typical run. The microphones were covered with thin plastic bags to protect them against water damage when not used for data taking. This photo shows the location of microphone number 3 and will serve to show the clutter of hard surface reflectors that caused the scattering of data for this microphone location. A large metal box was constructed to act as a water reservoir, and the water flow rate was then varied by changing the static head above the weir. Figure 3 shows a test engineer preparing to calibrate the water flow rate. Water flow-rate ratios of 1.0, 1.5, 2.0, 3.0, 3.33, 5.0, and 6.0 were tested as well as the dry condition. Free field measurements were also taken to find the effects of the flare bucket on both the near and far field attenuation.

ACOUSTIC MEASUREMENTS

A block diagram of the acoustical instrumentation is shown in Figure 4a. A sketch of the microphone locations appears as Figure 5. A photograph of the test equipment installation appears as Figure 6. A basic microphone, pre-amplifier and power supply is repeated for each channel. The Altec condenser microphones were laboratory calibrated prior to the test using a Western Electric 640 AA microphone as a reference standard. The General Radio portable calibrator was used both before and after each day of testing in the field.

The tape recorder output was fed through the analysis system shown in Figure 4b. Electronic calibration signals placed onto the tape at the time of data recording were fed through the analysis system and used as reference levels. All sound pressure levels* (SPL's) are well within the linear range of the microphones. The Ampex model 601-2 tape recorder is a two-channel machine. Because run times were limited to 10 to 15 seconds, the test conditions had to be repeated three times to gather data from all microphones. Initial tests showed the data to be repeatable to within $\pm$ 1 db so this method of data collection is believed to yield consistent results.

---

* Sound pressure level (SPL) in decibels is equal to 20 log $\frac{p}{p_o}$ where p is the rms sound pressure being measured and p_o is the reference pressure of 0.0002 dyne/cm^2.

Visual observation of the water spray pattern when the flame bucket was in operation indicated that it would not be possible to place the microphones in all necessary locations to probe the acoustic field and determine the acoustic power. Microphone number 1 was moved to an alternate location during this series of firings to prevent any possibility of damage from water blast. Figures 7 and 8 were taken in sequence during the operation of the flame bucket. Figure 7 was taken just before the gates were pulled with the flame bucket operating dry. Compare the relatively stable surface of the water reservoir in this figure with the highly turbulent surface as shown in Figure 8 after the gates were pulled. It appears that the water and rocket exhaust were mixing in the area of the weir. This mixing process is rather unsteady and might account for the turbulence. Apparently the high velocity efflux from the flame bucket caused water to be aspirated from the water reservoir.

Analysis of the data from microphone number 3 showed a considerable amount of scatter. This microphone was then tested and found to be in good working order. This scatter is believed to be a result of poor field conditions since there were many possible acoustic reflectors located near the microphones as previously mentioned. Microphone number 3 was kept as a spare, and the data will not be presented in this report.

Although no direct comparisons of total power reductions are possible, the present results should give indications of the potentials offered by direct water injection into the flame bucket.

DISCUSSION AND TEST RESULTS

A recent paper by Cole, England and Powell (Reference 3) discusses the effect of various exhaust blast deflectors on the acoustic characteristics of a small rocket engine. They observed that although the use of flame deflectors lowered the acoustic power in the far field, higher sound pressure levels were observed in the near field close to the rocket. This would be explained by a change in location of the effective sound source and the new acoustic field caused by the altered flow pattern.

Figure 9 has been taken from Reference 3 and is included to indicate the expected reduction in acoustic power through the use of this type of flame deflector. A comparison of results for both free-field and dry flame bucket configurations is shown in Figure 10. Microphone number 2 is well within the near field of the rocket engine and shows the marked dependence of SPL on distance in that regime. All of the spectra presented in this figure display a marked peak in the 1200-2400 cps band. This is in good agreement with the generalized data presented in Reference 4 when the frequency is presented in non-dimensional form as a Strouhal number. The Strouhal number $= f_m \frac{d}{U}$, where f_m is the mean geometric frequency of a particular octave band, d is the rocket exit diameter in feet, and U the rocket exhaust mean velocity in feet/second.

Figures 11 to 15 present octave band SPL's for all field locations where good data was obtained. Figure 11a shows that reductions in the order of 12 db in the near field are possible with a water flow-rate ratio of only 2.0/1. It is interesting to note that increasing the water flow-rate ratio to 6.5/1 did not yield any further noise reductions in this octave band. A similar trend is seen for microphone number 5 (radial distance 40 feet) although

the optimum water flow-rate ratio for this octave band has shifted to 3.33/1 (See Figure 14b). Note that for conditions in the far field, at least, increasing the water flow past the optimum condition resulted in an increase in SPL. This effect was more noticeable in the 1200-2400 cps band where peaking in the data was observed before. This same information is presented in another form in Figure 16 to 20 where SPL's from various microphone locations are plotted as a function of water flow-rate ratio. Both oberall and octave band data are presented.

A series of close-up photographs of flame bucket performance was taken during the test and are presented in Figures 21 through 24. These photographs show dry operation and water flows of 1.0/1, 2.0/1 and 2.0/1, respectively. These same close-up scenes may be seen in a short film made of these tests (Reference 5).

Figure 25 will serve as the first of a set of 3 summary plots. Overall sound pressure levels are plotted as a function of water flow-rate ratio for microphones 1, 2, 4 and 5. This figure shows that different water flow rates will prove optimum for various distances under consideration. This same information is presented in Figure 26 plotted as a function of radial distance from the flame bucket. Note that doubling the distance from the microphone resulted in a 6 db drop of sound pressure level. This would be indicative of far field locations. Microphone number 2 (at a distance of 5 feet from the flame bucket exhaust) and microphone number 5 (at a distance of 40 feet) were located on the same ray from the flame bucket. Microphone number 4 was located well below its ideal location (if it were to be on this same ray) and the data reflects the non-uniform acoustic field.

Figure 27 shows the sound pressure level relative to dry operation for a number of different water flows. This information is presented

as a function of the dimensionless frequency parameters (Strouhal number). Data from large rocket engines (Reference 4) show a peak in the sound pressure level spectrum for Strouhal numbers of 0.02 to 0.04. Figure 27 indicates a reduction of approximately 10 db in the noise level for this range of frequencies.

The basic theory of Lighthill (References 6 and 7) predicts the sound power of turbulent jets to vary as

$$P \sim \frac{\rho_j^2 d^2 U^8}{\rho_o c_o^8}$$

ρ_j = mean density of the jet
ρ_o = mean density of free stream
d = diameter of the nozzle
U = mean velocity of the jet
c_o = mean speed of sound in the free stream

This theoretical result does not account for high speed flows where the turbulent jet becomes supersonic.

Data presented by Powell (Reference 8) indicates that the exponent of velocity is reduced from a value of 8 for low speed flow to a value of 3 for supersonic speeds. The pressure amplitude in the near field of rocket exhaust becomes great enough to cause non-linear effects thereby invalidating the classical acoustic theory.

Experimental data indicates that the efficiency of noise production of a turbulent jet varies as the fifth power of the jet Mach number, U/c_o. However, this relation could not be expected to hold for large scale rocket engines, for at a Mach number of six, all of the kinetic energy of the jet would be converted into acoustic energy.

The data indicates that this efficiency approaches a value of 1% of the mechanical power of the jet for large engines. A complete theoretical explanation of these empirical observations is not available at this time. However, it might be possible to make several observations about the experiment being reported upon in this report.

The reduction in noise level due to direct injection of water into the flame bucket may be examined in relation to changes in the properties of the flow. A transfer of thermal energy between the exhaust gases and the water stream causes steam to be generated with the resultant lowering of the gas temperature and change in density of the exhaust stream. Turbulent mixing will occur between the gas stream and the water which in turn lowers the jet velocity considerably. The flame bucket acts as a diffuser which in turn lowers the exit velocity of the stream. However, this tends to increase the effective exit area of the jet stream.

There also is the possibility of a spectral change in the rocket noise as a function of water flow. This would arise from the change in effective jet velocity and its effect on the noise generating mechanism. Previous experiments (Reference 9) indicate the spectra to be flatter for lower speeds. Octave band data presented in this report is not adequate to determine whether such a change took place. Additional narrow-band data reduction would be required to determine the peak frequency present in the sound spectrum.

Density and temperature effects on the efficiency of jet noise production are still in question. References 7, 9, and 11 indicate that these effects are small when compared to the turbulent pressure fluctuations of the jet mixing process. Lighthill (Reference 6) shows, however, that a maximum value of 6 db might be expected for very hot jets. This result is a theoretical one in which the effects of both temperature and density variation are related to the

adiabatic pressure change. The hot gas temperature is reflected in a local mean velocity of sound. This increased noise should occur in the higher octave bands. Lighthill notes that the combustion process itself should not be overlooked as a contributor to the total noise of the rocket engine.

The reason for an optimum water flow-rate ratio for far field noise reduction is not clearly understood at this time. The use of a gravity head in the water reservoir would indicate that a finite mixing rate would occur between the rocket exhaust and the cooling water. It might be possible that when the water flow rate exceeded this optimum value, the mixing process was not allowed to proceed to completion and excessive turbulence occurred at the weir. This turbulence is an additional noise source in itself. The increased reservoir head and water flow in the flame bucket could act as an acoustic reflector, thus causing higher near-field sound pressure levels in the higher frequencies and result in possible combustion instability of the rocket engines.

As a final check on the flame bucket performance, the engines were started while the bucket was completely flooded. This was done to simulate failure of the weir system. The bucket cleared itself of excess water, and normal operation was then observed. There were no acoustic measurements taken, however, because the water spray pattern was unknown and damage to the microphones was feared if left uncovered.

CONCLUSIONS AND RECOMMENDATIONS

This test was exploratory in nature and was done to determine whether realistic reductions in noise levels would be achieved by direct water injection with the flame bucket. The results obtained show promise for both near and far field noise reduction. The flame bucket performed well during the entire series of tests. The gates operated smoothly and no hot-spots were observed on the bucket after any of the tests.

The explanation of an optimum water flow-rate ratio for far field noise reduction is not possible at this time. The mechanism of noise reduction is complex and can only be described by experimental results.

It is recommended that these studies be extended to provide additional information necessary for construction of full-scale flame buckets. Further data reduction will be required on data taken during the present series of tests to determine the extent of any shift in noise spectrum as a function of water flow-rate ratio.

The water reservoir should be enlarged and the weir system redesigned. The present configuration allows excess water to be aspirated into the flame bucket during the run which causes the water level to drop in the reservoir. This in turn causes a drop in water flow-rate ratio during the run.

The acoustic field should be probed to determine the acoustic power of the rocket engine-flame bucket combination.

Additional large-scale tests are necessary to test the validity of Strouhal type scaling laws for rocket noise. Lighthill (Reference 7) observed that the additional noise due to high temperature flow occurs

in the higher frequencies. The present tests showed that the noise due to the turbulent jet occurred in the same octave band. It is possible that larger scale engines might show a broader band type of noise reduction since the frequencies of the turbulent flow noise would appear in a lower octave band.

Far field noise reduction studies are concerned with energy present in the lower octave bands (20-75, 75-150 and 150-300 cps). Data gathered in this test indicate the greatest potential to occur in this range of frequencies for the large scale booster rockets currently being designed. However, a word of caution is suggested in using a simple Strouhal type of scaling law to extrapolate data until further investigated.

REFERENCES

1. Hendershot, K. C., "Design and Operation of 1/30 Scale Atlas Booster and Sustainer Rocket Engines", Convair San Diego Division Report RT-401, 4 March 1960.

2. To be Published by Thermo Test Lab. GD/Convair (Description of Flame Bucket).

3. Cole, England and Powell, "Effects of Various Exhaust Blast Deflectors on the Acoustic Noise Characteristics of 1,000-Pound-Thrust Rockets", WADD TR 60-6, September 1960.

4. Cole, Von Gierke, et. al., "Noise Radiation From Fourteen Types of Rockets in the 1,000 to 130,000 Pounds Thrust Range ", WADD TR 57-354, Dec. 1957.

5. Motion Picture Section, "Noise Suppression Tests", Cat. No. 114-9389-5624 General Dynamics/Astronautics, 31 August 1961.

6. Lighthill, M. J., "On Sound Generated Aerodynamically, Part I, General Theory", Proc. Roy, Soc., Vol. A 211, pp 564-587, 1952.

7. Lighthill, M. J., "On Sound Generated Aerodynamically, Part II, Turbulence as a Source of Sound", Proc. Roy, Soc., Vol. A 222 pp 1-32, 1954.

8. Powell, A., "On the Generation of Noise by Turbulent Jets", ASME paper 59-AV-53, March 1959.

9. Powell, A., "Theory and Experiment in Aerodynamic Noise with a Critique of Research on Jet Flows and Their Relation to Sound", Office of Naval Research Second Symposium on Naval Hydrodynamics, July 1958.

10. Powell, A., "A Schlieren Study of Small Scale Air Jets, and Some Noise Measurements on Two-Inch Diameter Jets", Aero Research Council Paper 14726, 1951.

11. Rollins, V. G., "Effects of Temperature on Jet Noise Generation", NACA TN 4217, 1958.

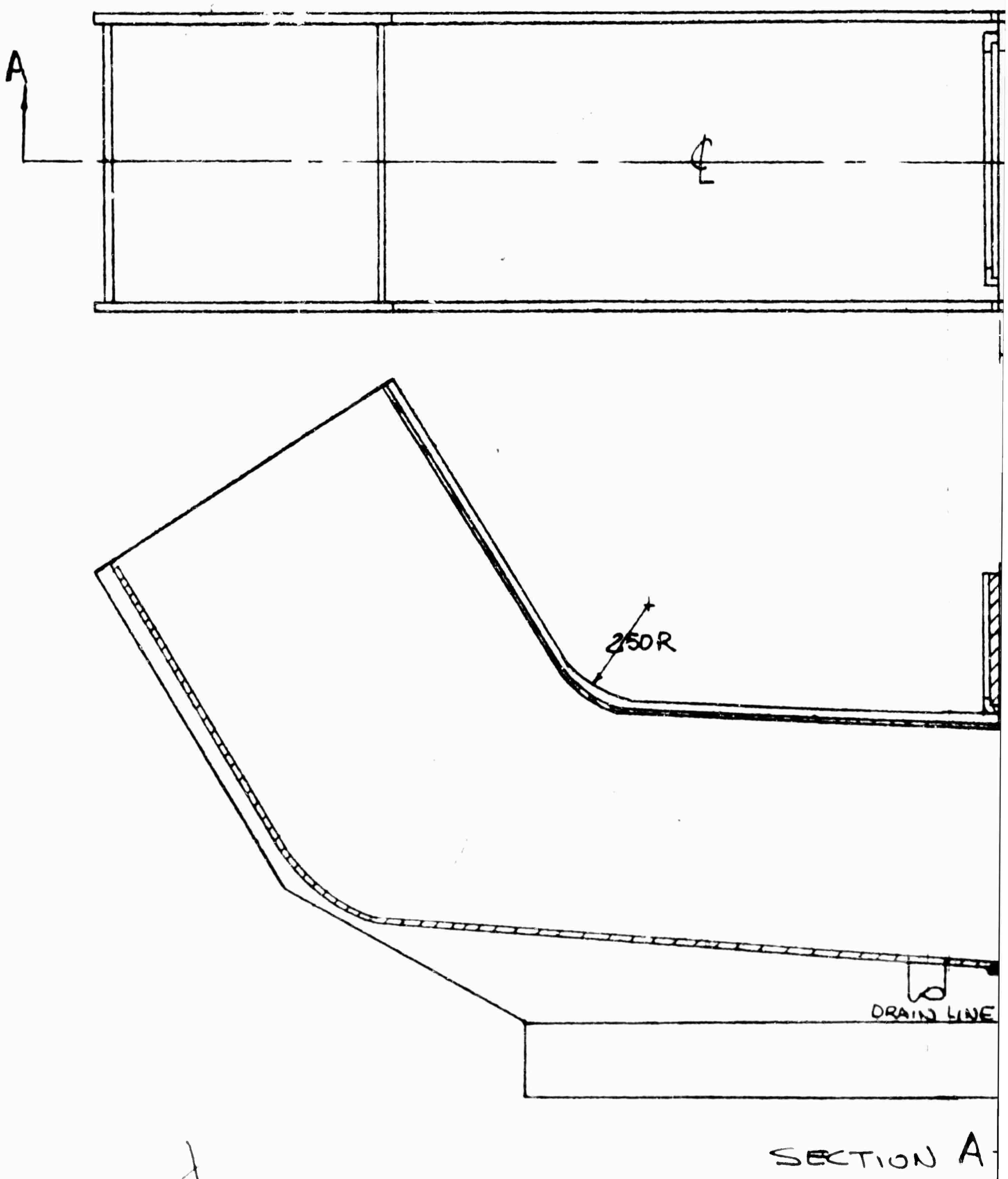

SECTION A

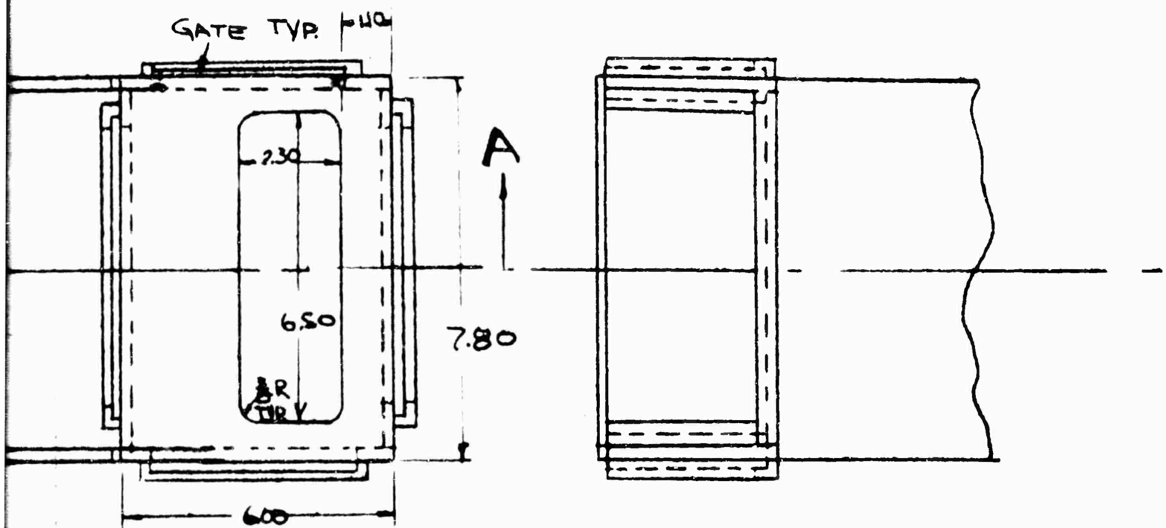

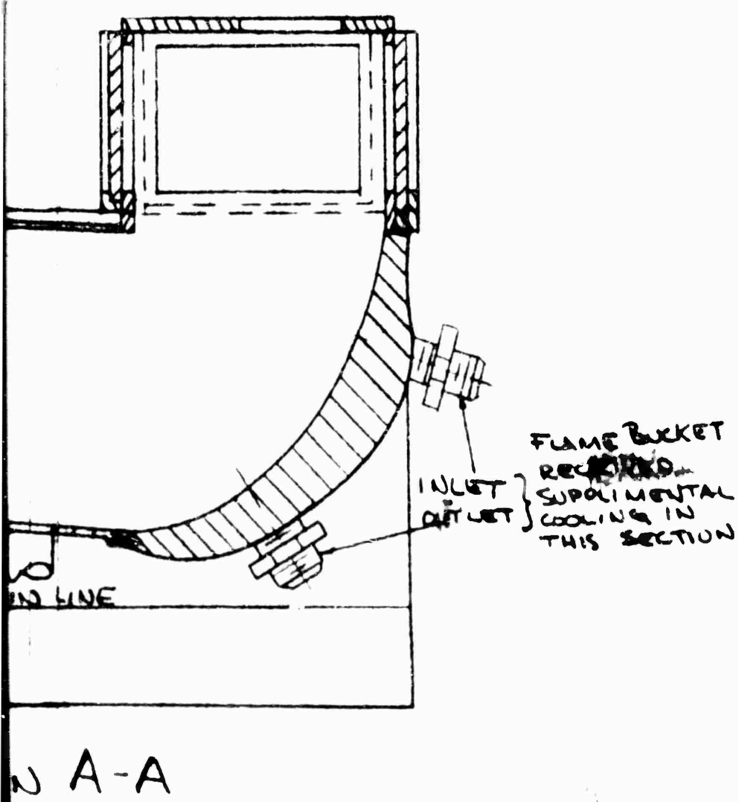

WATER COOLED FLAME BUCKET
DESIGNED BY: GD/CONVAIR THERMO-
DYNAMICS LAB
TL R&D 1089
SCALE: —
DATE: AUGUST 26, 1961

Figure 1

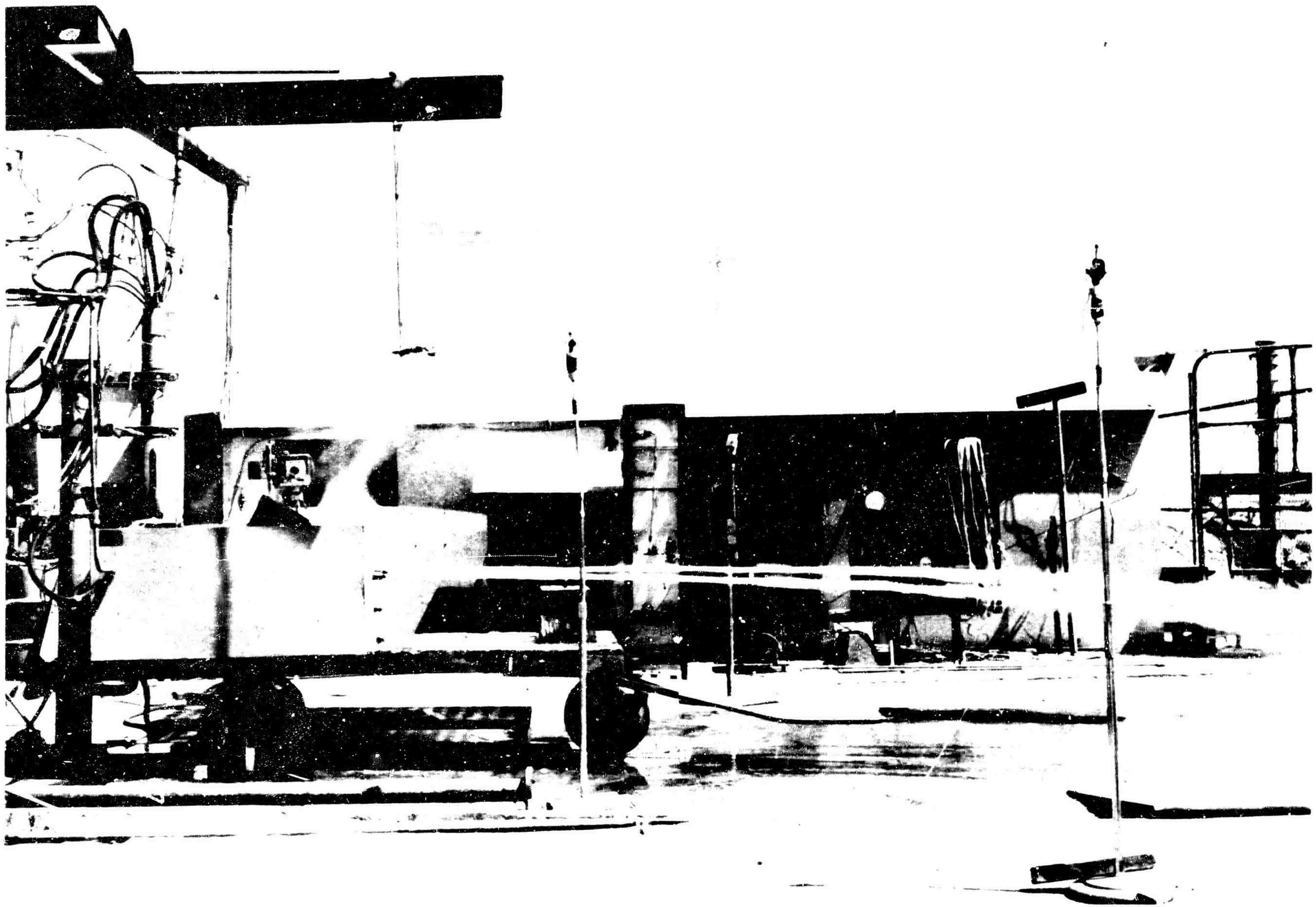

FIGURE 2 Overall View of Test Site During Typical Run

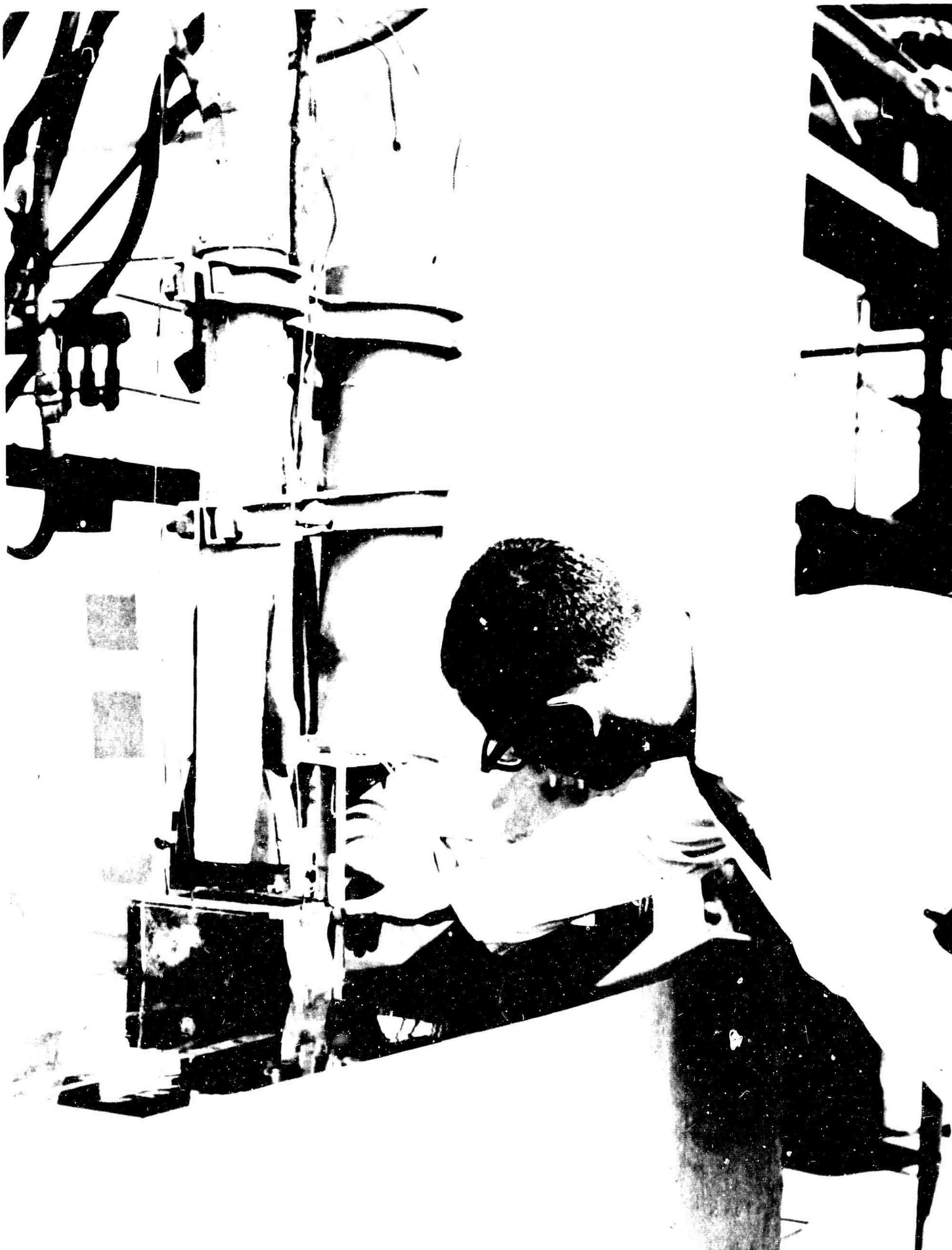

FIGURE 3 Measurement of Reservoir Static Head

Acoustical Measurement Instrumentation

Recording

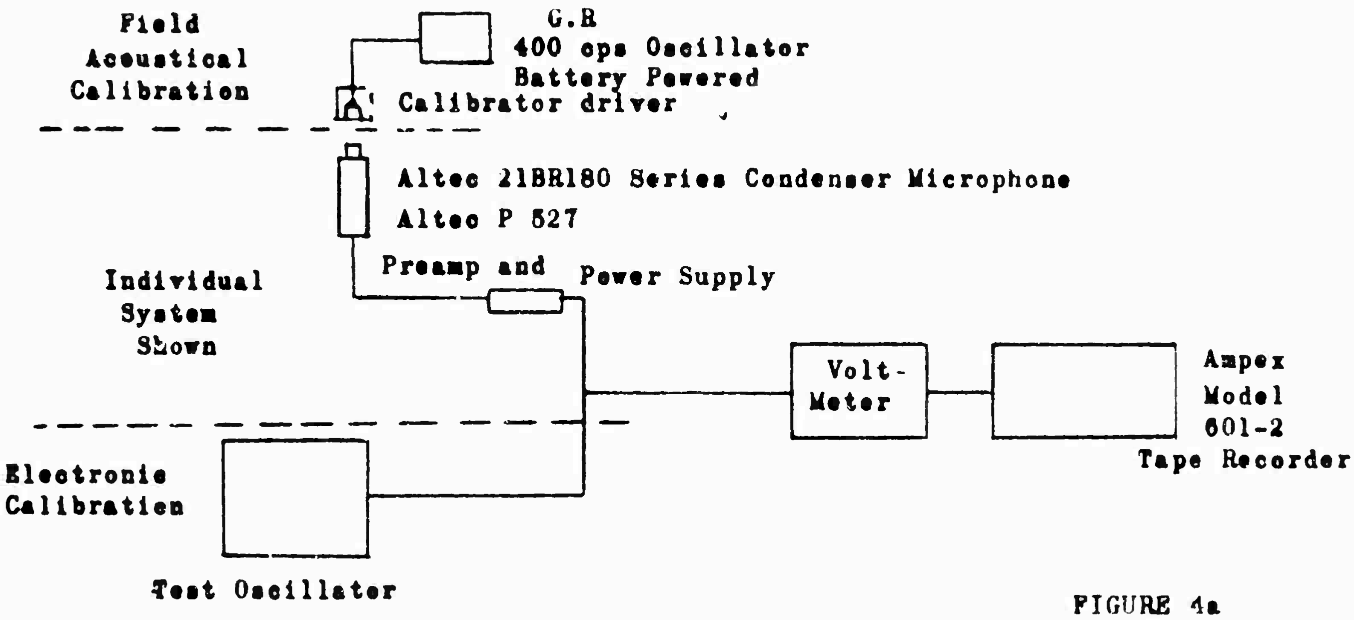

FIGURE 4a

Analysis

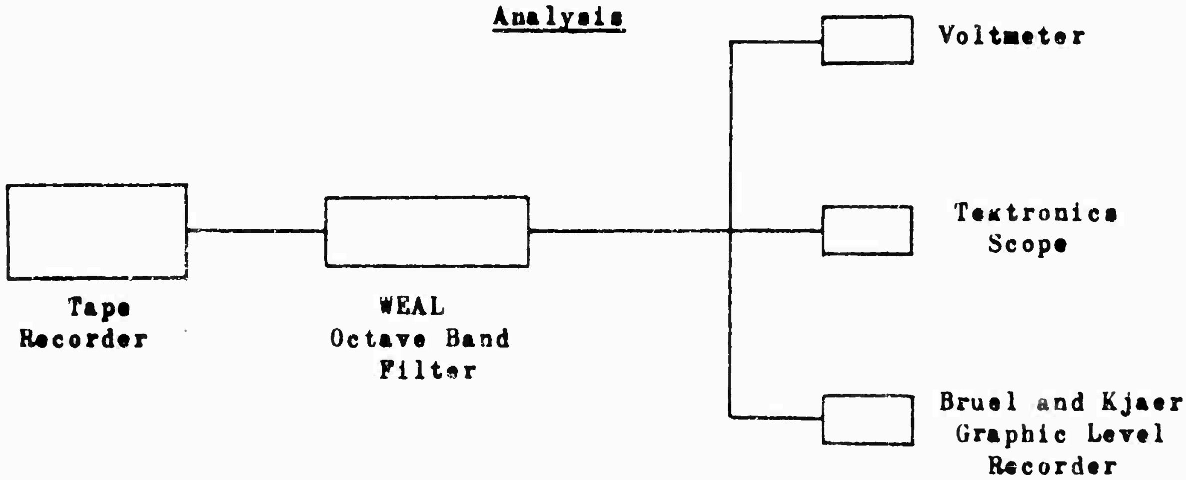

FIGURE 4b

MICROPHONE LOCATIONS

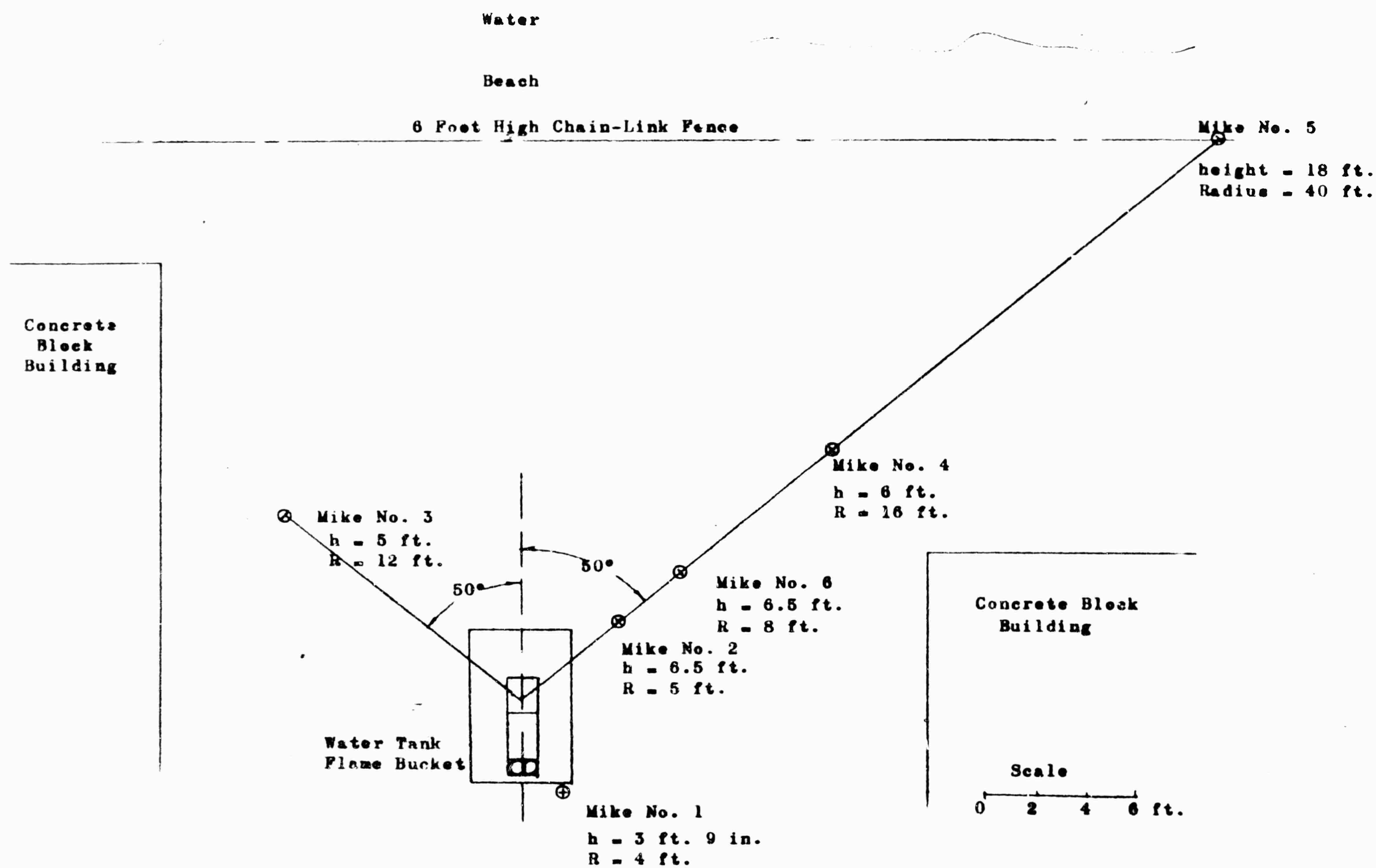

FIGURE 5

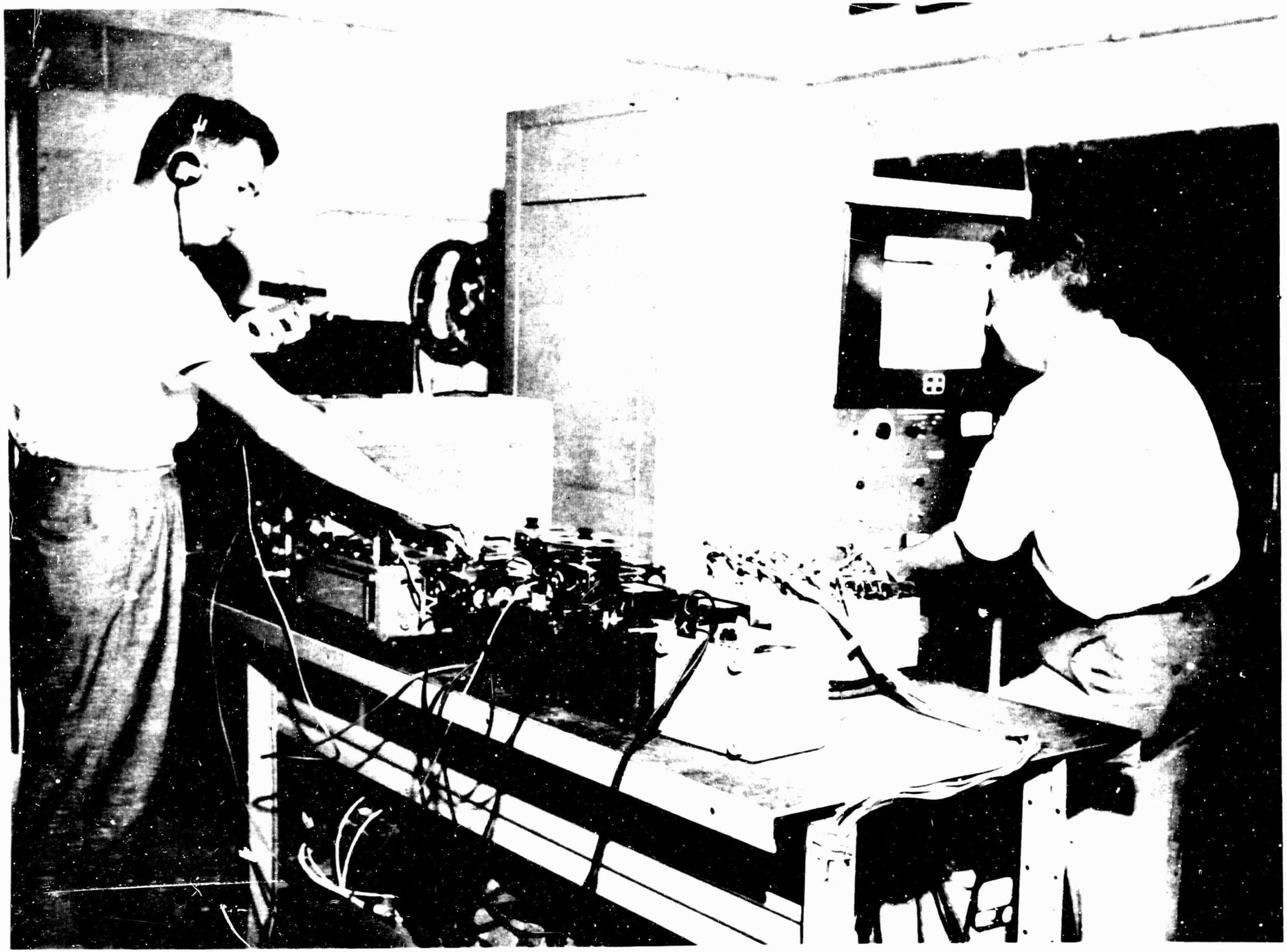

FIGURE 6 Test Equipment Installation

NOT REPRODUCIBLE

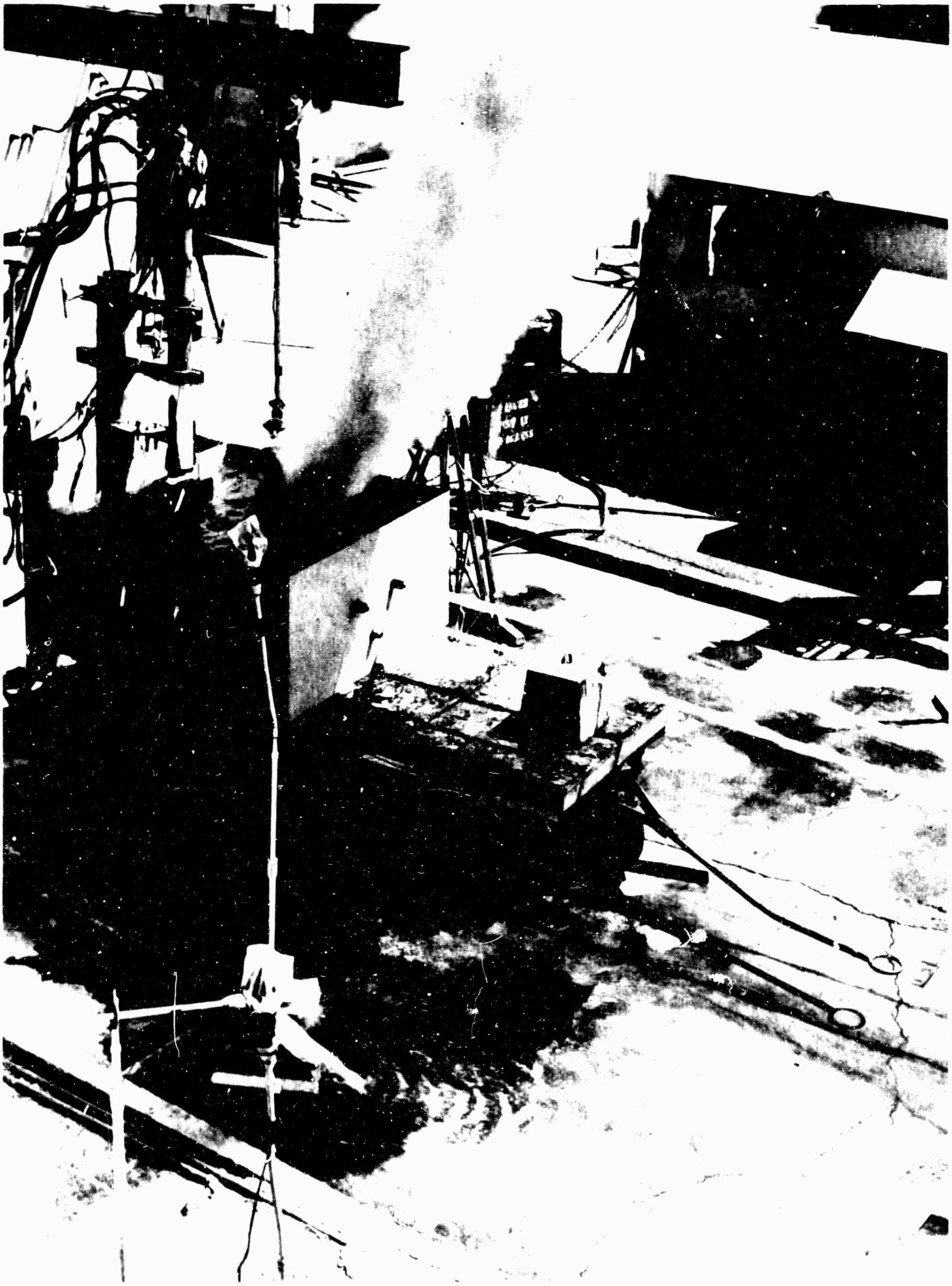

FIGURE 7 Flame Bucket Operating Dry

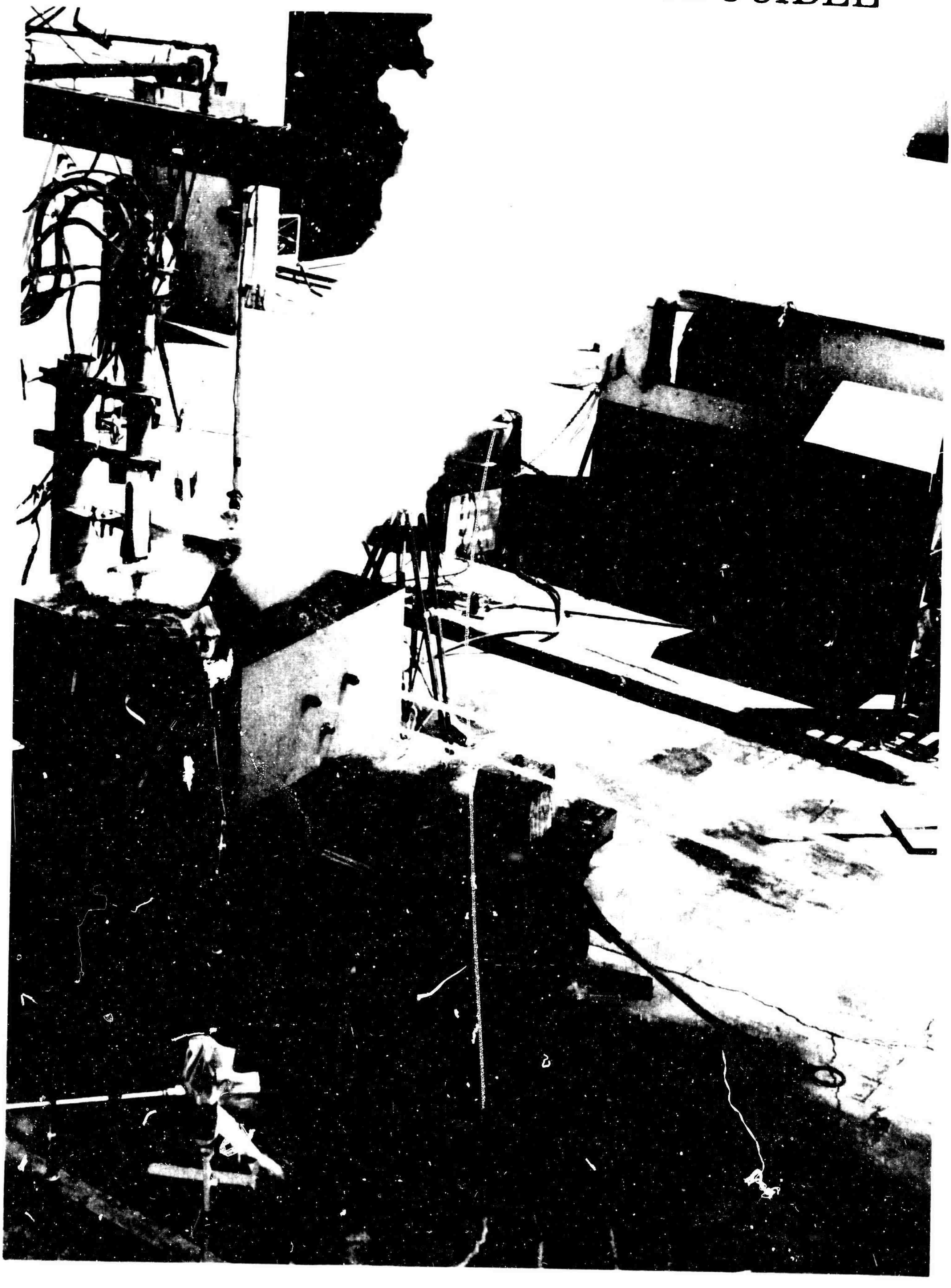

FIGURE 8 Flame Bucket Operating with Water Flow

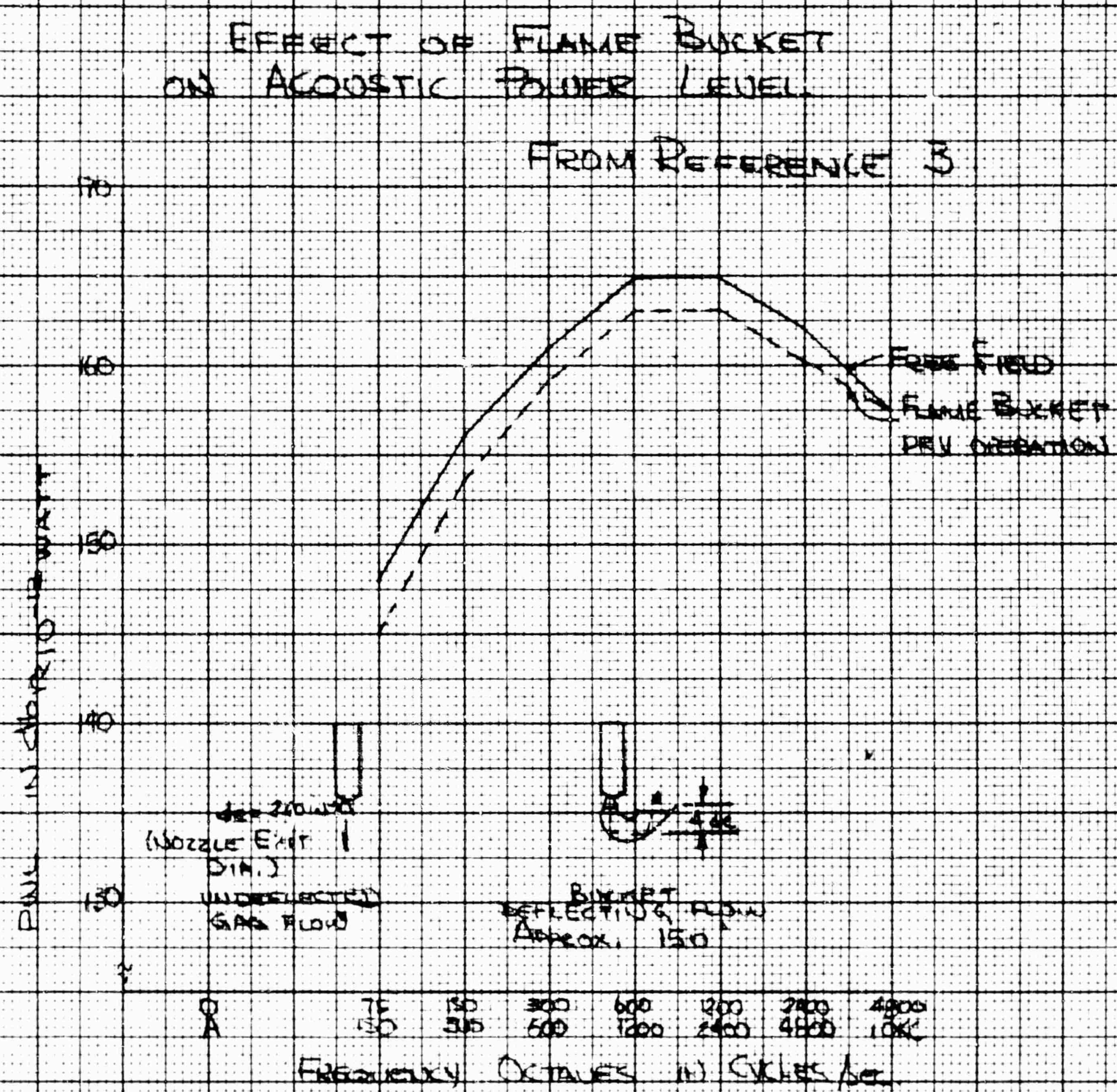
EFFECT OF FLAME BUCKET
ON ACOUSTIC POWER LEVEL
FROM REFERENCE 3
FREE FIELD
FLAME BUCKET
DEV. OPERATION
PWL IN db RE 10^{-12} WATT
FREQUENCY OCTAVES IN CYCLES/SEC.
UNDEFLECTED
GAS FLOW
BUCKET
DEFLECTING FLOW
APPROX. 150

FIGURE 9

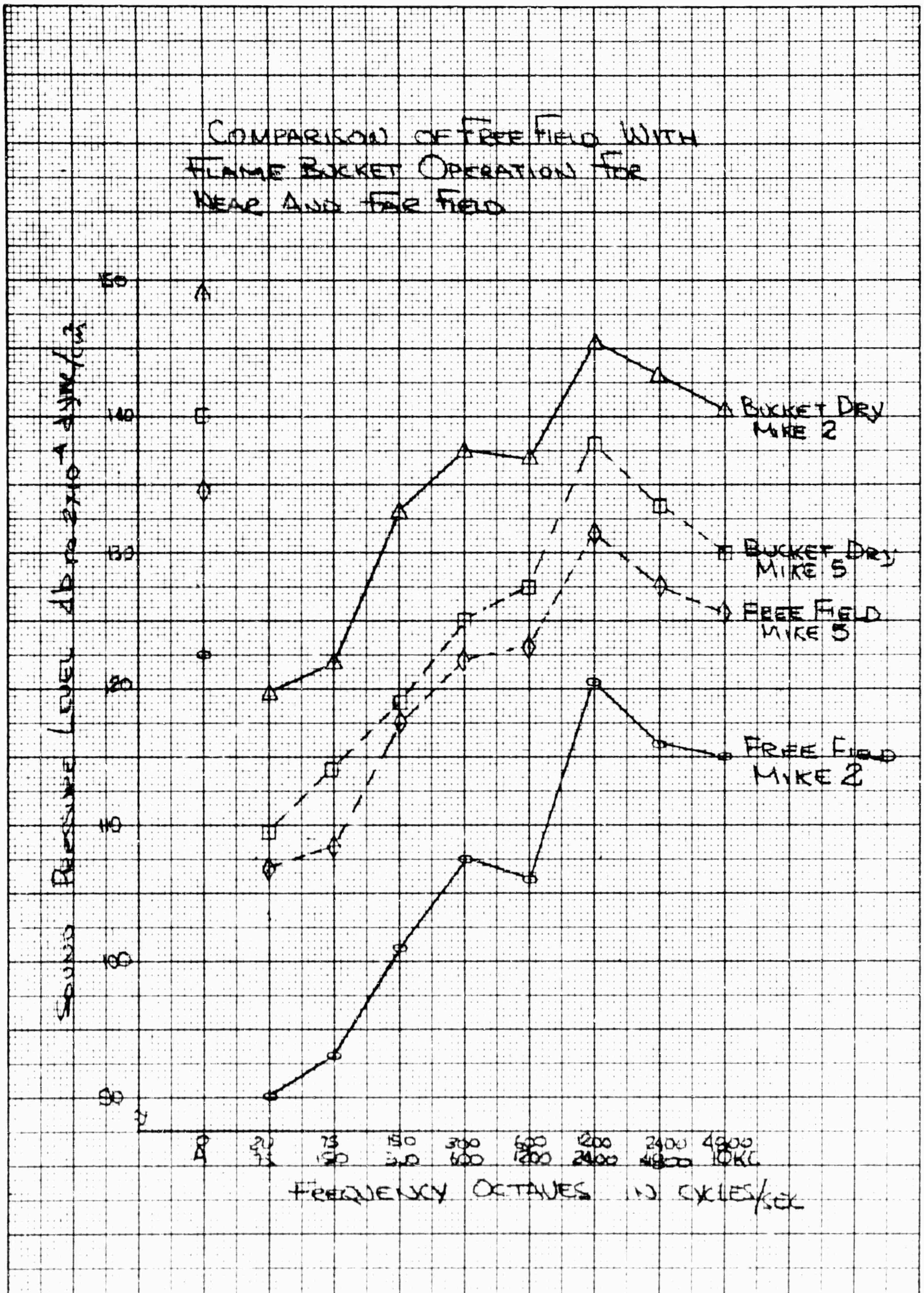
COMPARISON OF FREE FIELD WITH
FLAME BUCKET OPERATION FOR
NEAR AND FAR FIELD
SOUND PRESSURE LEVEL db re 2x10-4 dyne/cm2
FREQUENCY OCTAVES IN CYCLES/SEC
BUCKET DRY MIKE 2
BUCKET DRY MIKE 5
FREE FIELD MIKE 5
FREE FIELD MIKE 2
150
140
130
120
110
100
90
20 75
75 150
150 300
300 600
600 1200
1200 2400
2400 4800
4800 10KC

FIGURE 10

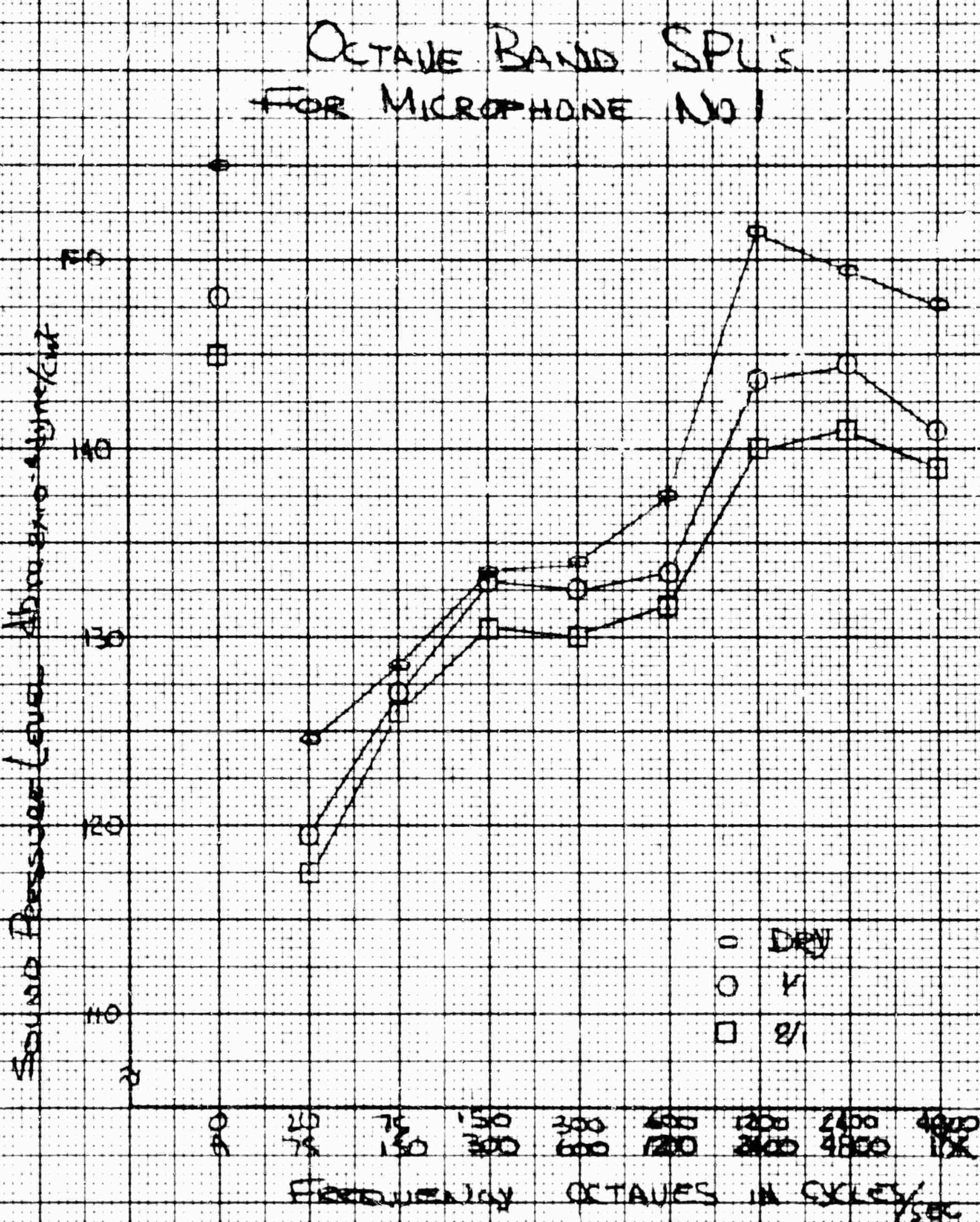
OCTAVE BAND SPL's
FOR MICROPHONE NO 1
150
140
130
120
110
Sound Pressure Level db re 0.0002 dyne/cm²
0 A
20 75
75 150
150 300
300 600
600 1200
1200 2400
2400 4800
4800 10K
FREQUENCY OCTAVES IN CYCLES/SEC
DRY
1/1
2/1

FIGURE II4

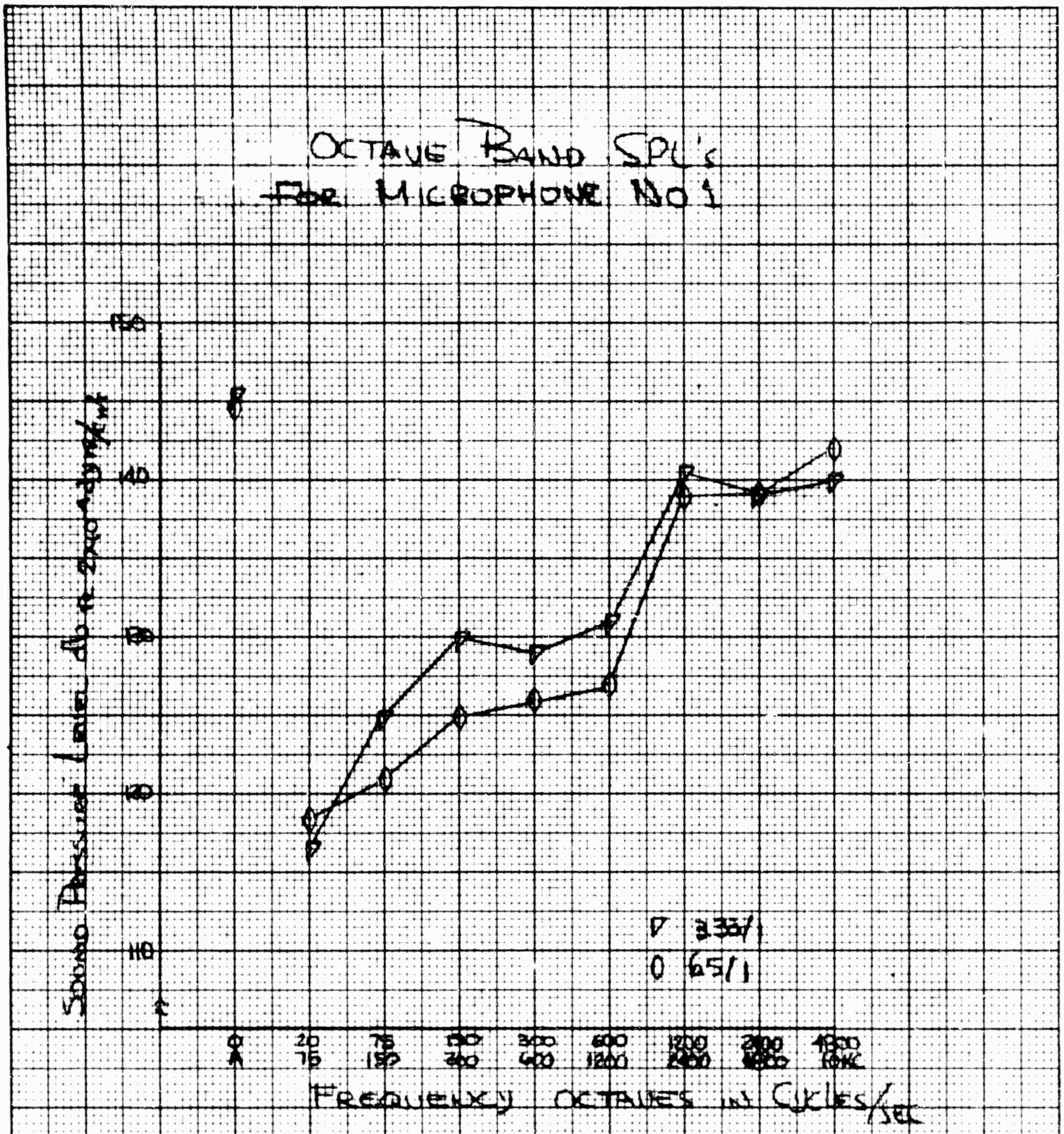
OCTAVE BAND SPL's
FOR MICROPHONE No 1
Sound Pressure Level db re 2x10⁻⁴ dynes/cm²
150
140
130
120
110
FREQUENCY OCTAVES IN CYCLES/SEC
A
20 75
75 150
150 300
300 600
600 1200
1200 2400
2400 4800
4800 10KC
∇ 33/1
0 65/1

FIGURE 11b

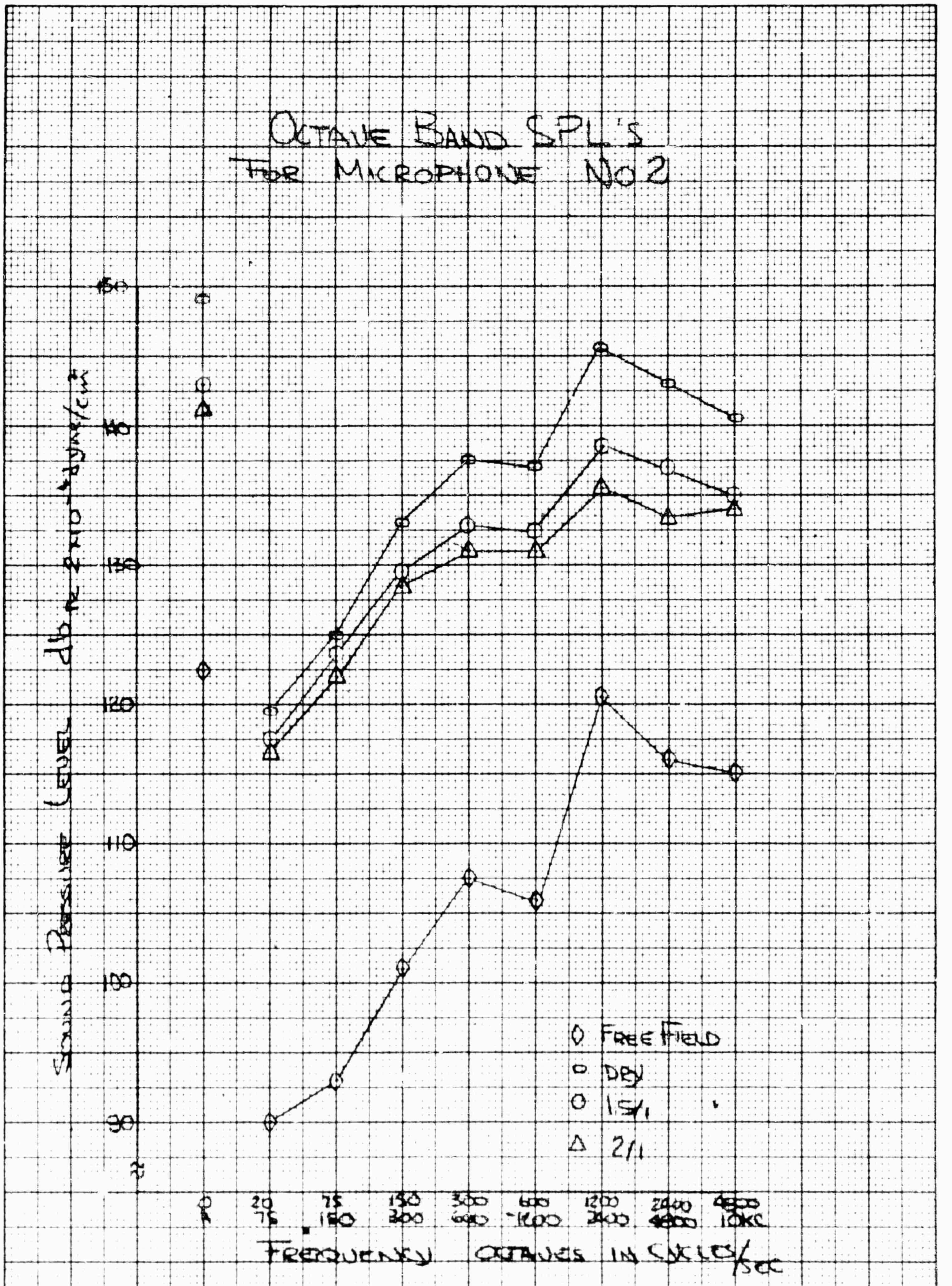
OCTAVE BAND SPL'S
FOR MICROPHONE NO 2
SOUND PRESSURE LEVEL db re 2x10⁻⁴ dyne/cm²
150
140
130
120
110
100
90
0 FREE FIELD
DRY
15/1
2/1
0
20 75
75 150
150 300
300 600
600 1200
1200 2400
2400 4800
4800 10KC
FREQUENCY OCTAVES IN CYCLES/SEC

FIGURE 12a

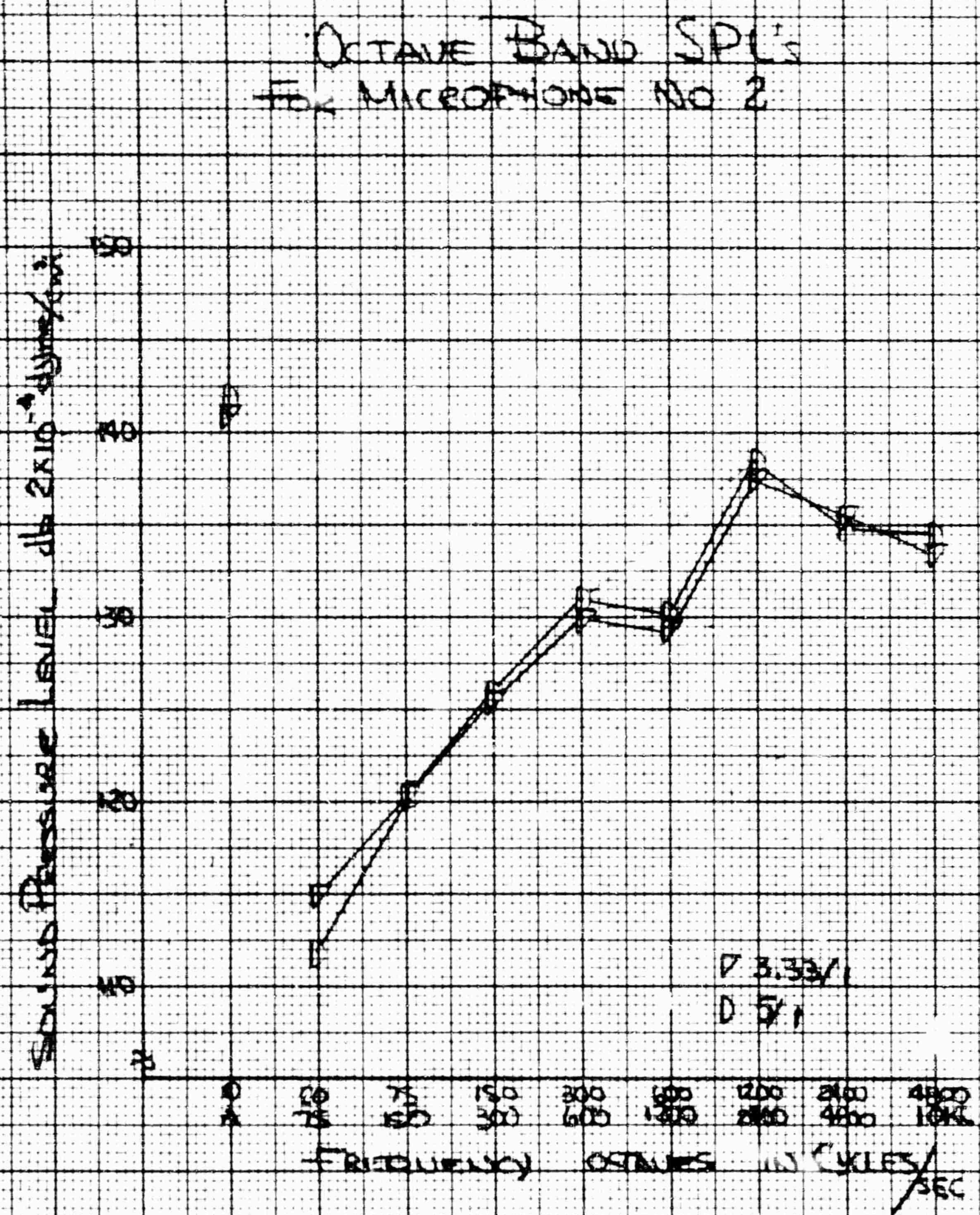
OCTAVE BAND SPL's
FOR MICROPHONE NO 2
SOUND PRESSURE LEVEL db 2X10^-4 dyne/cm²
150
140
130
120
110
10
20 75
75 150
150 300
300 600
600 1200
1200 2400
2400 4800
4800 10KC
▽ 3.33/1
□ 5/1
FREQUENCY OCTAVES IN CYCLES/SEC

FIGURE 18b

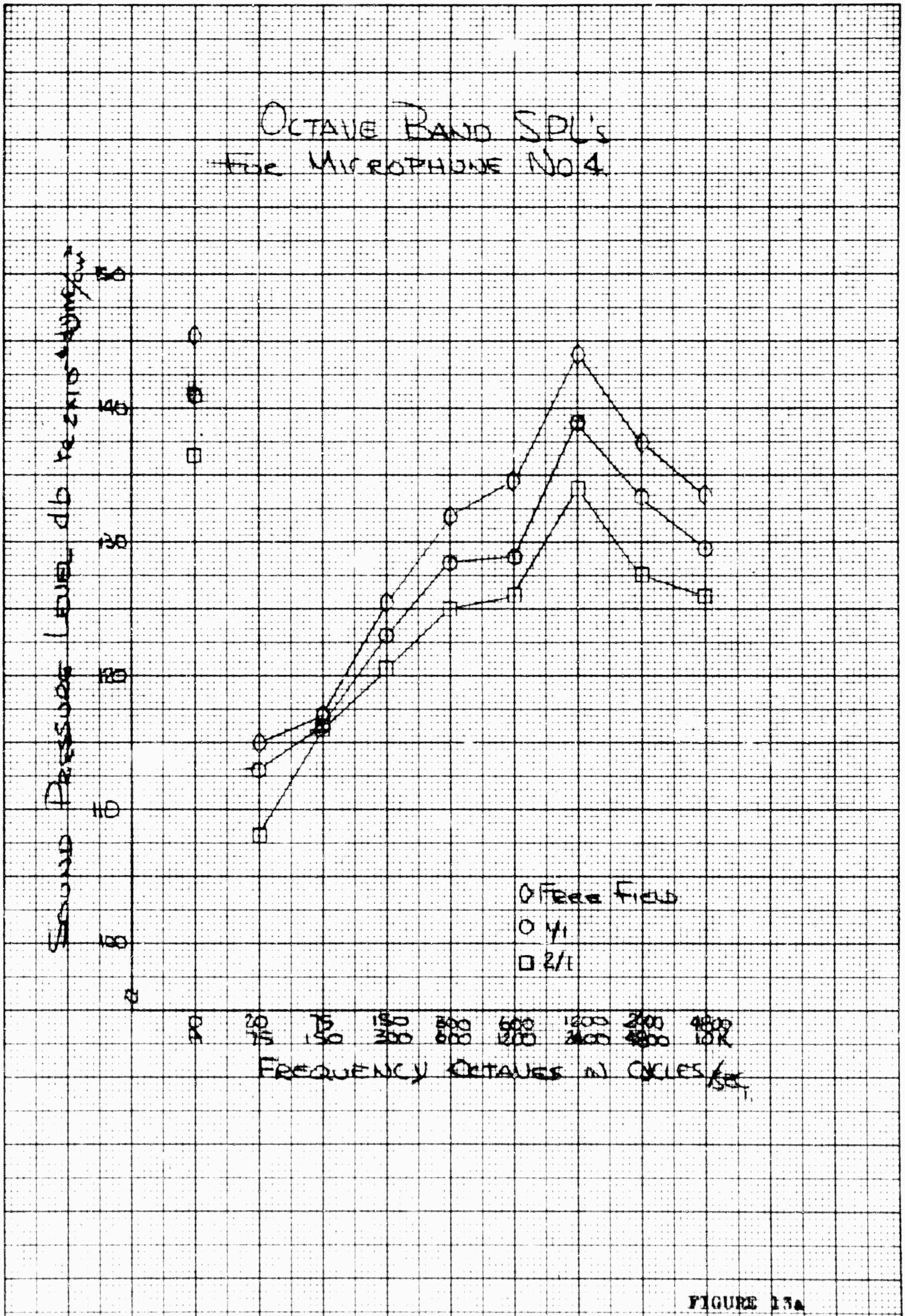
Octave Band SPL's
For Microphone No 4
Sound Pressure Level db re 2x10^-4 dyne/cm²
150
140
130
120
110
100
0
Frequency Octaves in Cycles/Sec
O Free Field
O 1/1
□ 2/1

FIGURE 13a

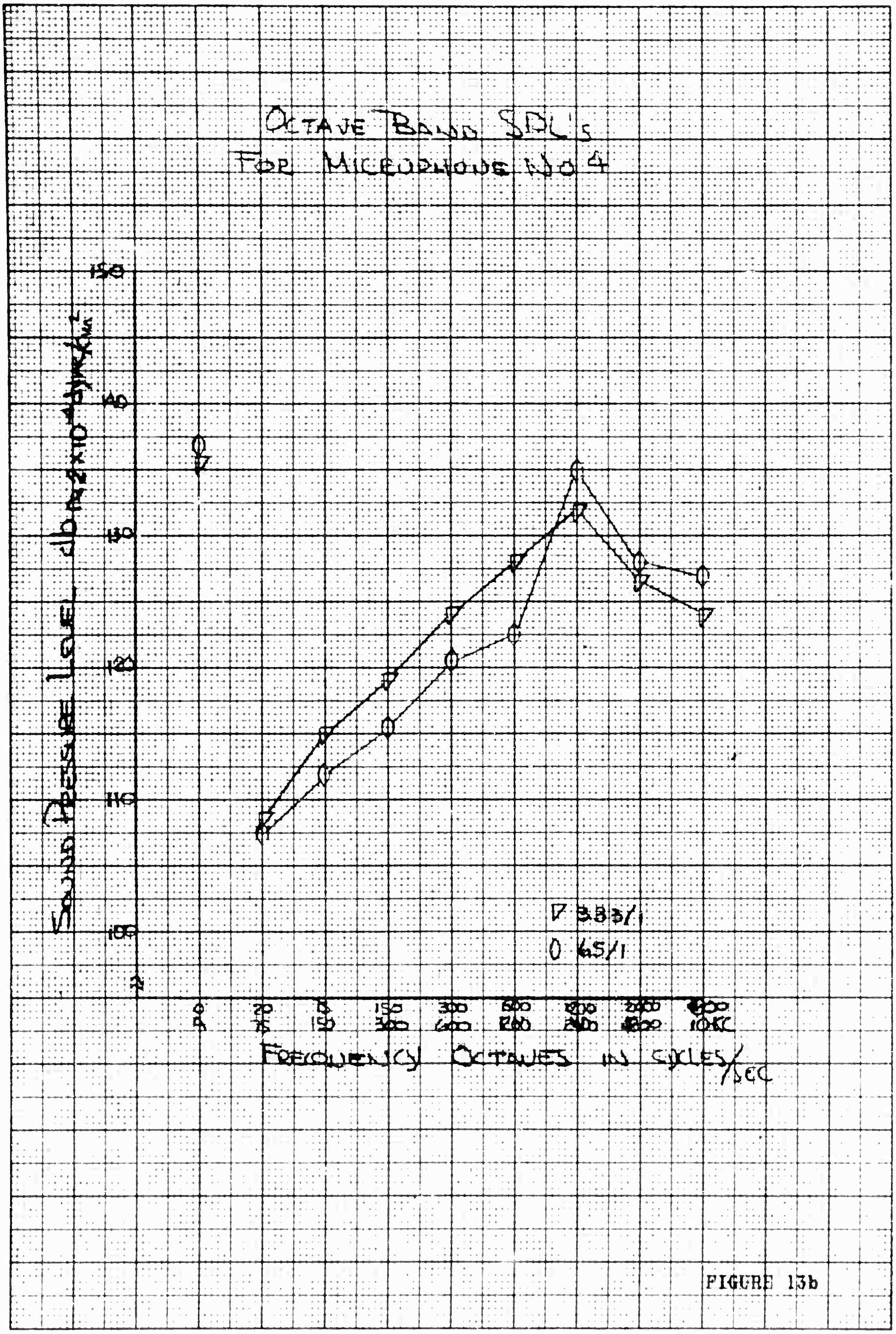
OCTAVE BAND SPL'S
FOR MICROPHONE NO 4
SOUND PRESSURE LEVEL db re 2x10⁻⁴ dyne/cm²
150
140
130
120
110
100
▽ 3.33/1
O 4.5/1
FREQUENCY OCTAVES IN CYCLES/SEC

FIGURE 13b

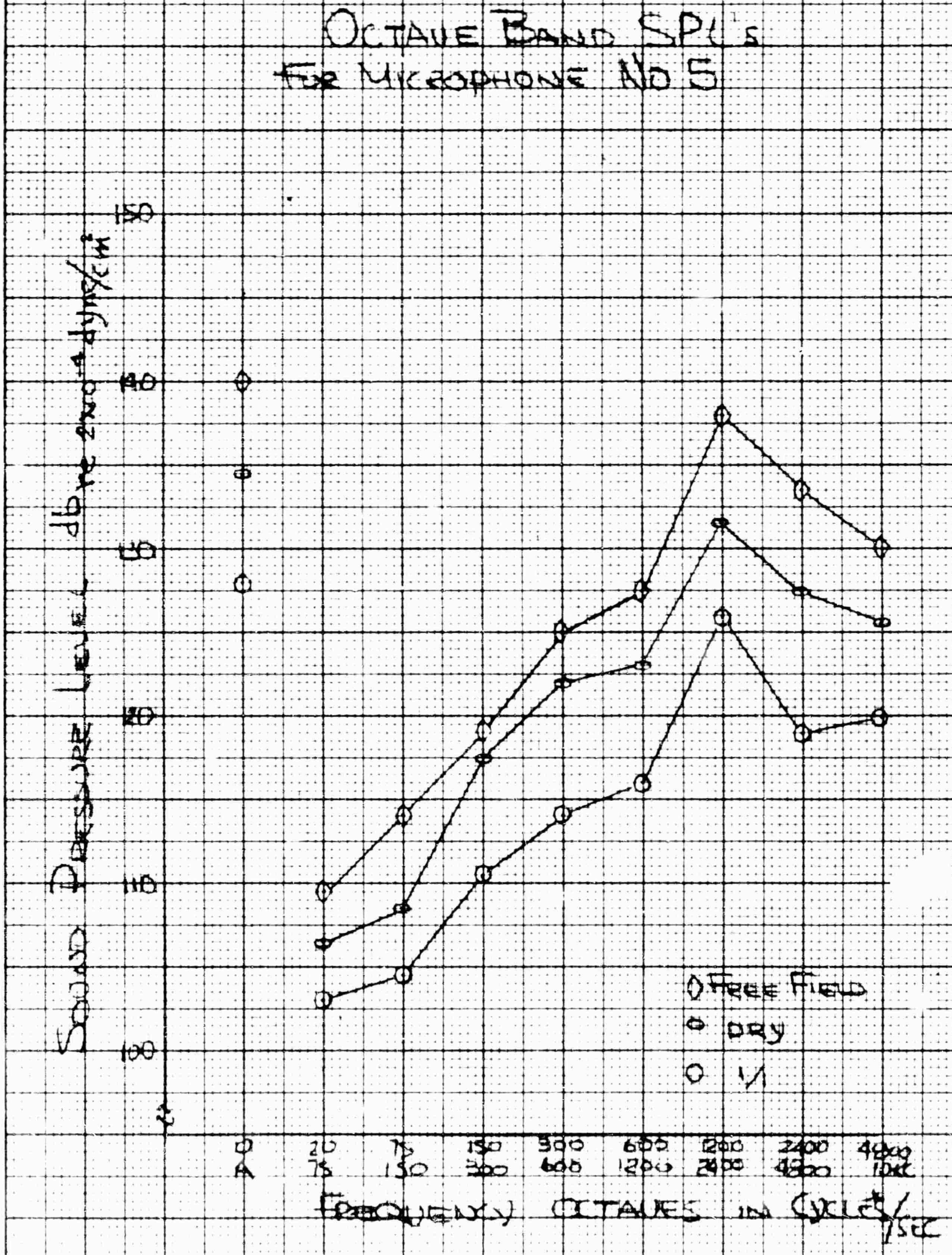
OCTAVE BAND SPL's
FOR MICROPHONE NO 5
SOUND PRESSURE LEVEL db re 2x10-4 dyne/cm2
150
140
130
120
110
100
0 A
20 75
75 150
150 300
300 600
600 1200
1200 2400
2400 4800
4800 10K
FREQUENCY OCTAVES IN CYCLES/SEC
FREE FIELD
DRY

FIGURE 14a

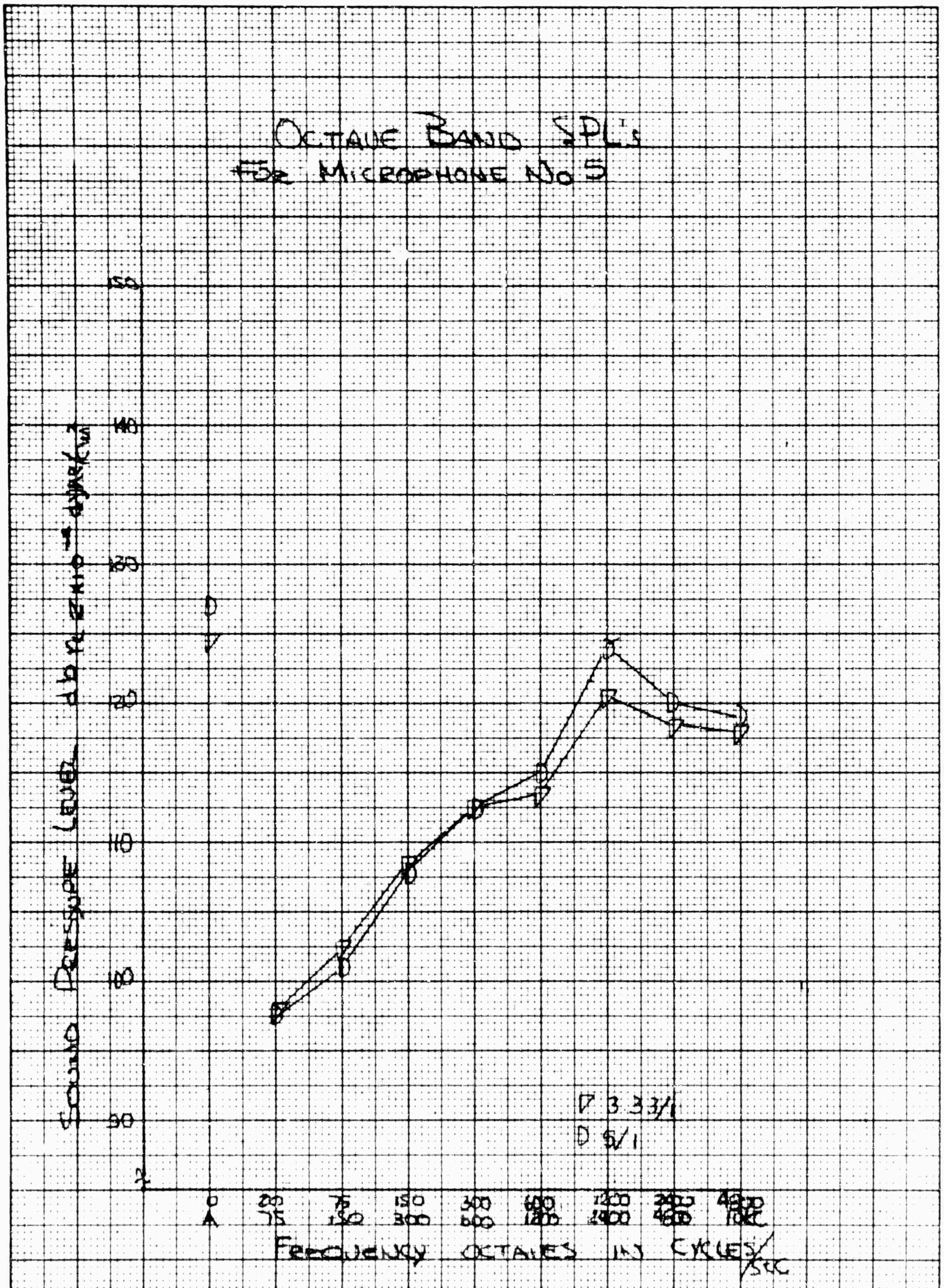
Octave Band SPL's
For Microphone No 5
Sound Pressure Level
150
140
130
120
110
100
90
0
A
20
75
75
150
150
300
300
600
600
1200
1200
2400
2400
4800
4800
10KC
Frequency Octaves in Cycles/Sec
3 3/1
5/1

FIGURE 14b

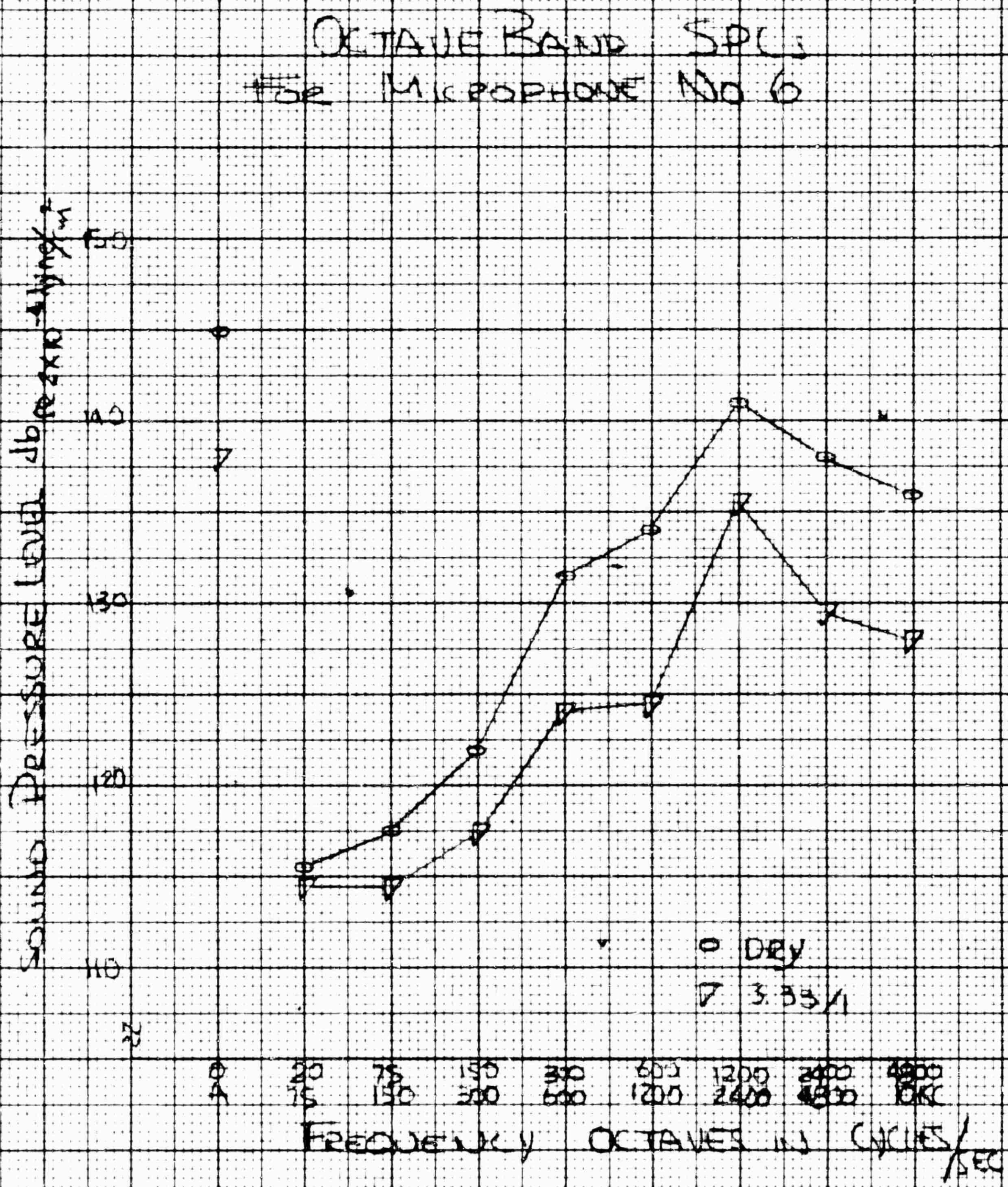
OCTAVE BAND SPL
#5e MICROPHONE No 6
SOUND PRESSURE LEVEL db re 2x10⁻⁴ dyne/cm²
150
140
130
120
110
0 A
20 75
75 150
150 300
300 600
600 1200
1200 2400
2400 4800
4800 10KC
FREQUENCY OCTAVES IN CYCLES/SEC
o Dry
▽ 3.35/1

FIGURE 15

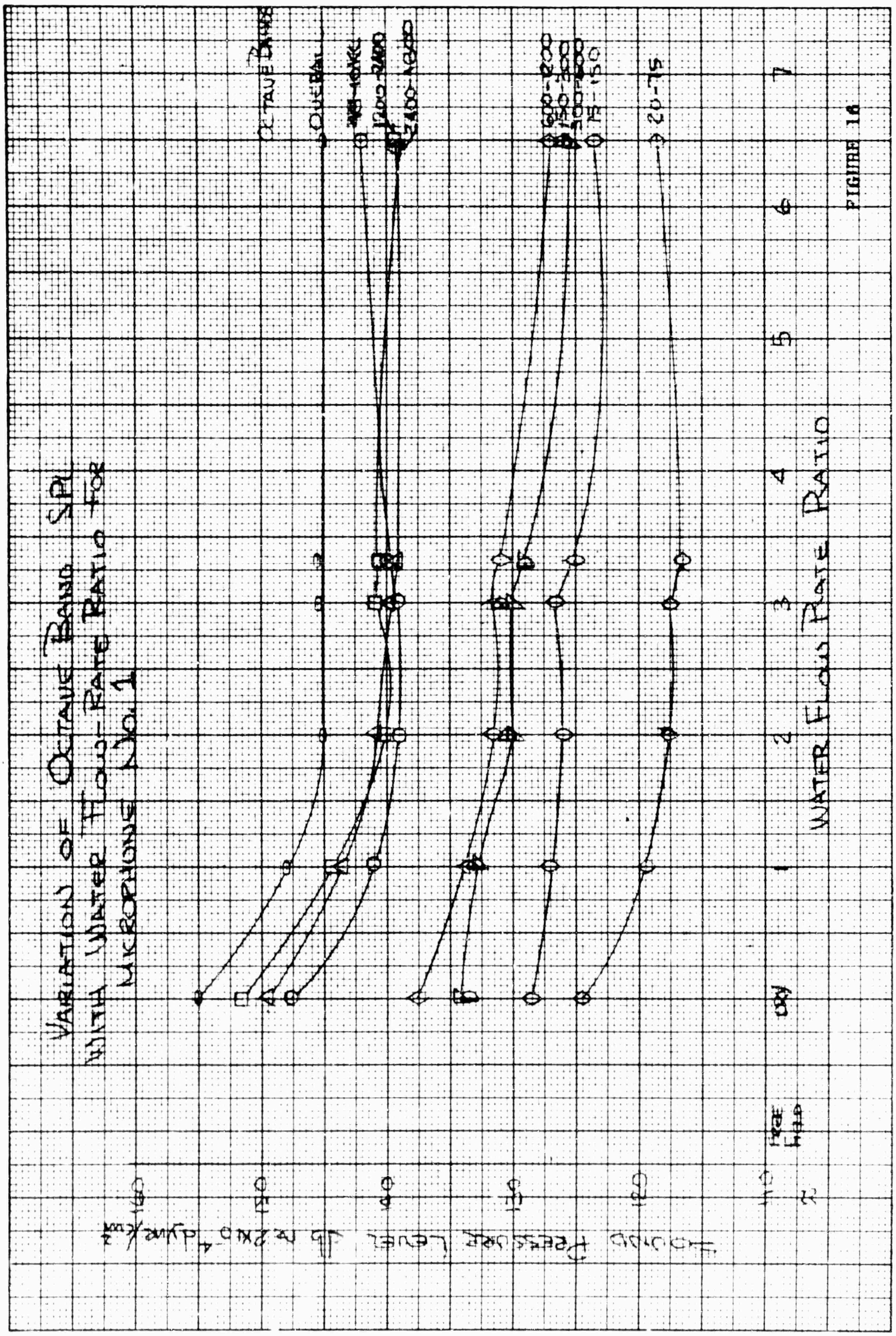
VARIATION OF OCTAVE BAND SPL
WITH WATER FLOW-RATE RATIO FOR
MICROPHONE NO. 1
OCTAVE BANDS
OVERALL
4800-10000
1200-2400
2400-4800
600-1200
150-300
300-600
75-150
20-75
SOUND PRESSURE LEVEL db re 2x10^-4 dyne/cm²
WATER FLOW RATE RATIO
DRY
1
2
3
4
5
6
7
110
120
130
140
150
160

FIGURE 16

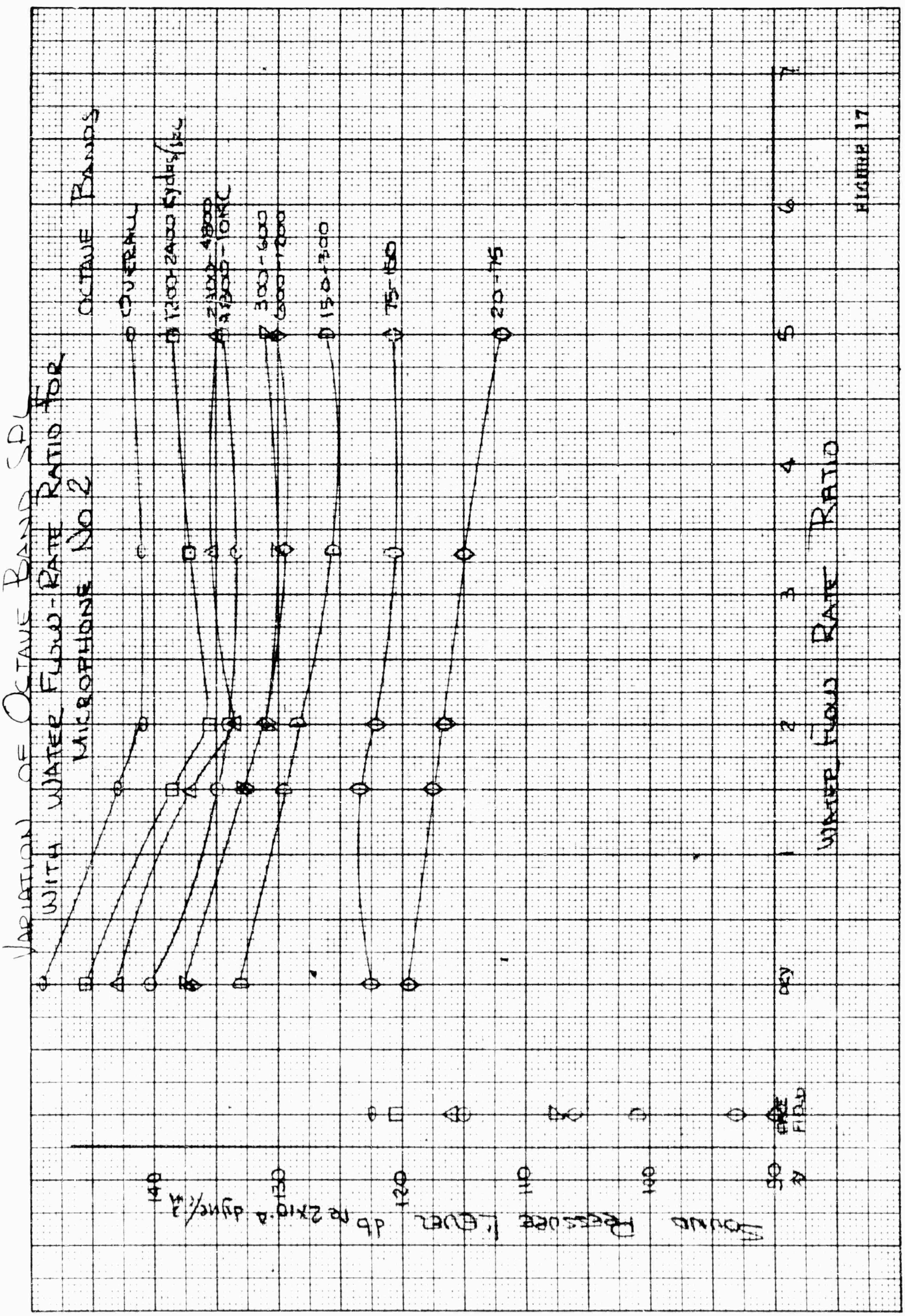
VARIATION OF OCTAVE BAND SPL
WITH WATER FLOW-RATE RATIO FOR
MICROPHONE NO 2
OCTAVE BANDS
OVERALL
1200-2400 Cycles/Sec
2400-4800
4800-10KC
300-600
600-1200
150-300
75-150
20-75
WATER FLOW RATE RATIO
DRY
1
2
3
4
5
6
7
FREE FIELD
Sound Pressure Level db re 2x10^-4 dyne/cm^2
140
130
120
110
100
90

FIGURE 17

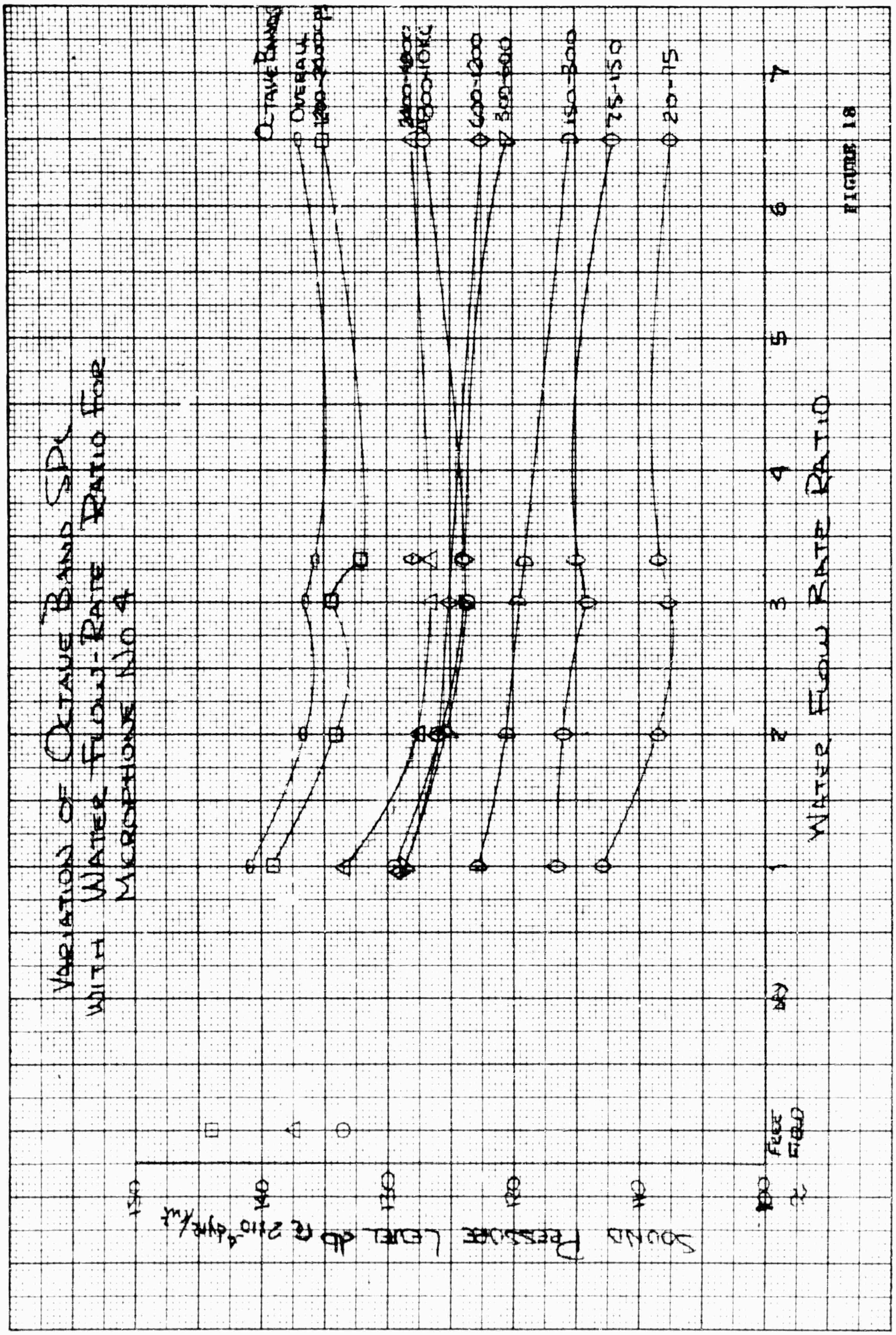
VARIATION OF OCTAVE BAND SPL
WITH WATER FLOW-RATE RATIO FOR
MICROPHONE NO 4
OCTAVE BANDS
OVERALL
1200-2400 CPS
2400-4800
4800-10KC
600-1200
300-600
150-300
75-150
20-75
SOUND PRESSURE LEVEL db re 2x10⁻⁴ dyne/cm²
150
140
130
120
110
100
FREE FIELD
DRY
1
2
3
4
5
6
7
WATER FLOW RATE RATIO

FIGURE 18

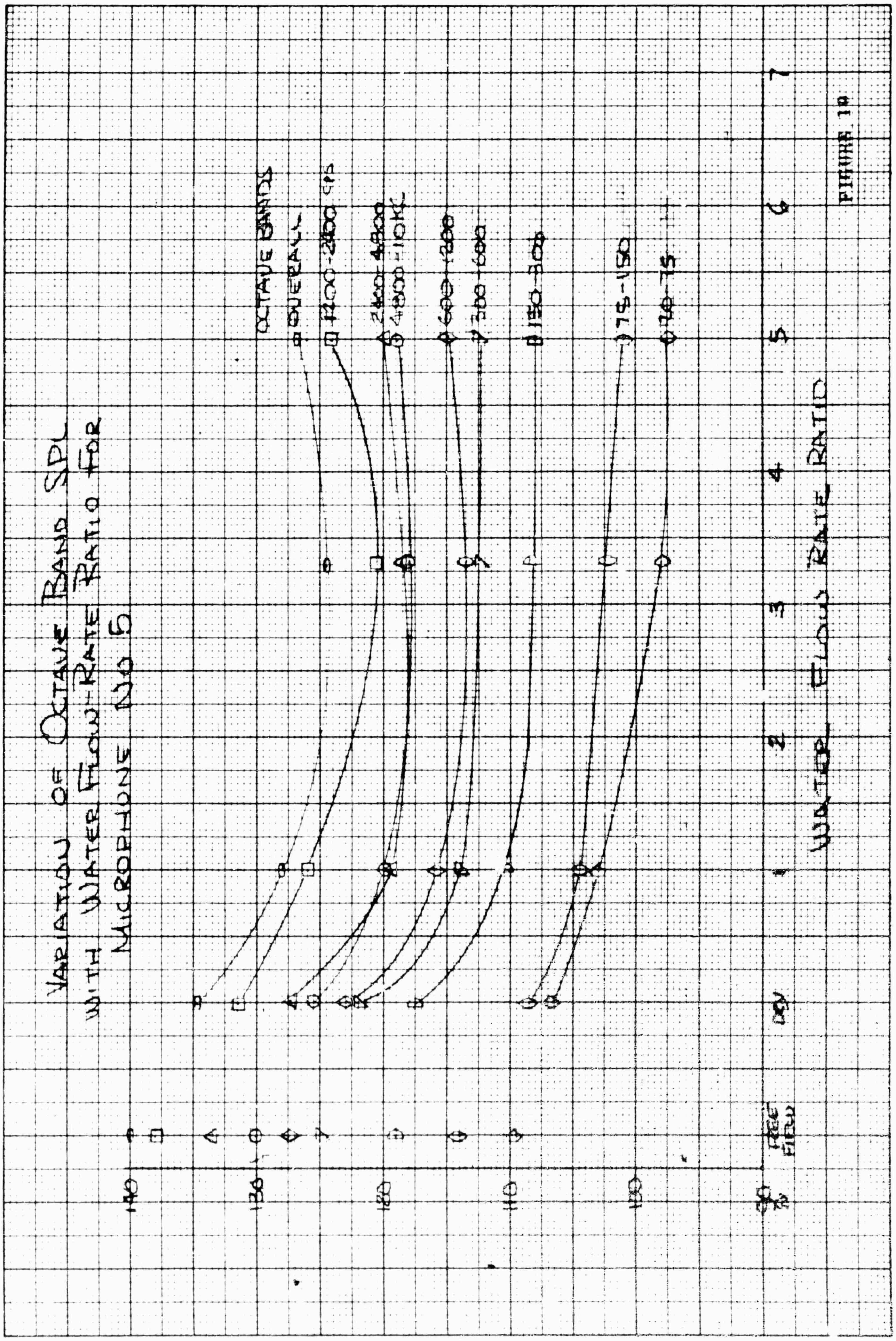
VARIATION OF OCTAVE BAND SPL
WITH WATER FLOW RATE RATIO FOR
MICROPHONE NO 5
OCTAVE BANDS
OVERALL
1200-2400 CPS
2400-4800
4800-10KC
600-1200
300-600
150-300
75-150
140
130
120
110
100
FREE FIELD
1
2
3
4
5
6
7
WATER FLOW RATE RATIO

FIGURE 19

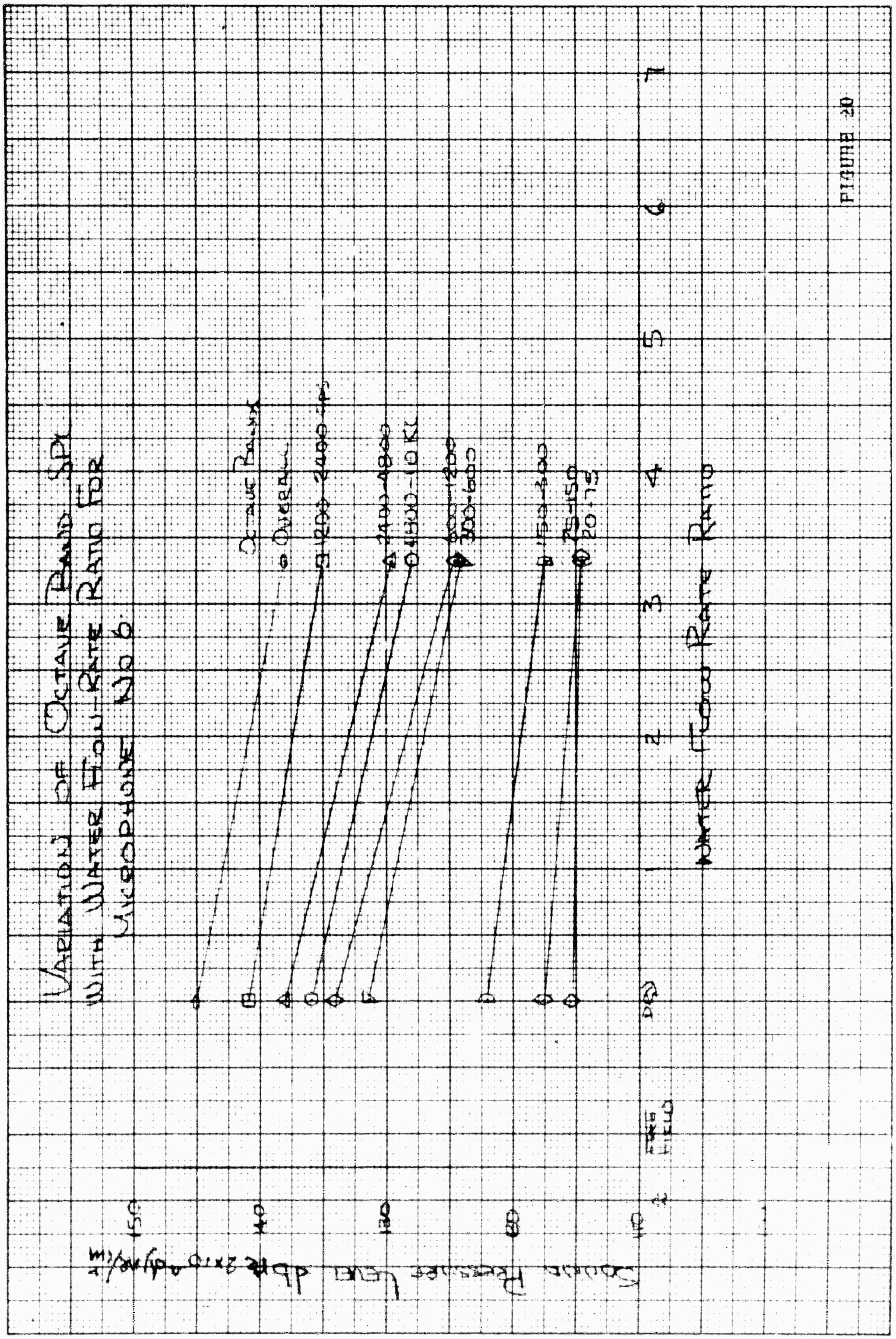
Variation of Octave Band SPL With Water Flow-Rate Ratio for Microphone No. 6
Octave Band
Overall
1200-2400 cps
2400-4800
4800-10 Kc
600-1200
300-600
150-300
75-150
20-75
Water Flow Rate Ratio
Sound Pressure Level dB re 2x10^-4 dyne/cm^2
150
140
130
120
110
Free Field
Dry
1
2
3
4
5
6
7

FIGURE 20

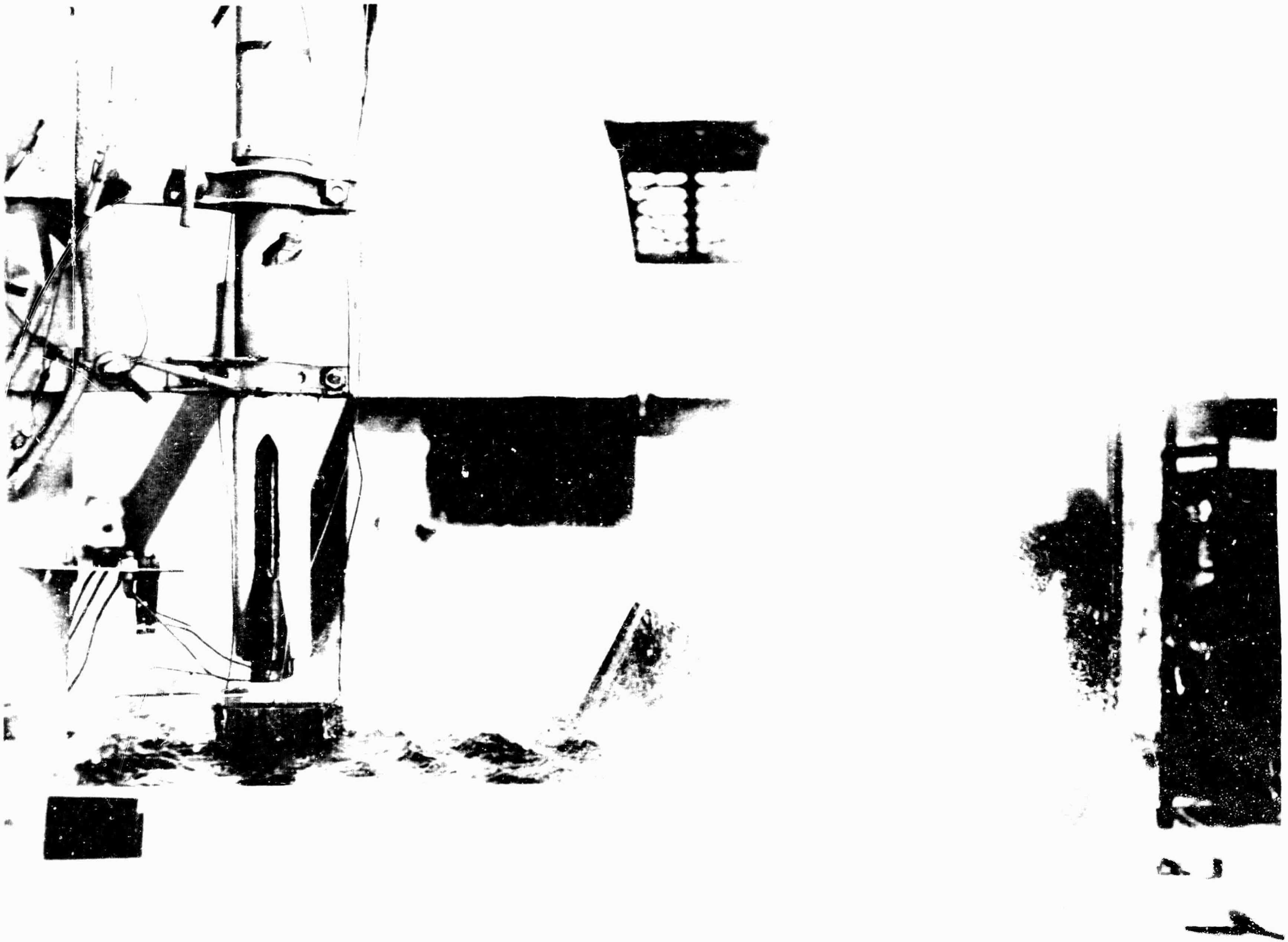

FIGURE 21 Flame Bucket Operation Dry Condition
AE61-1140 Page 38

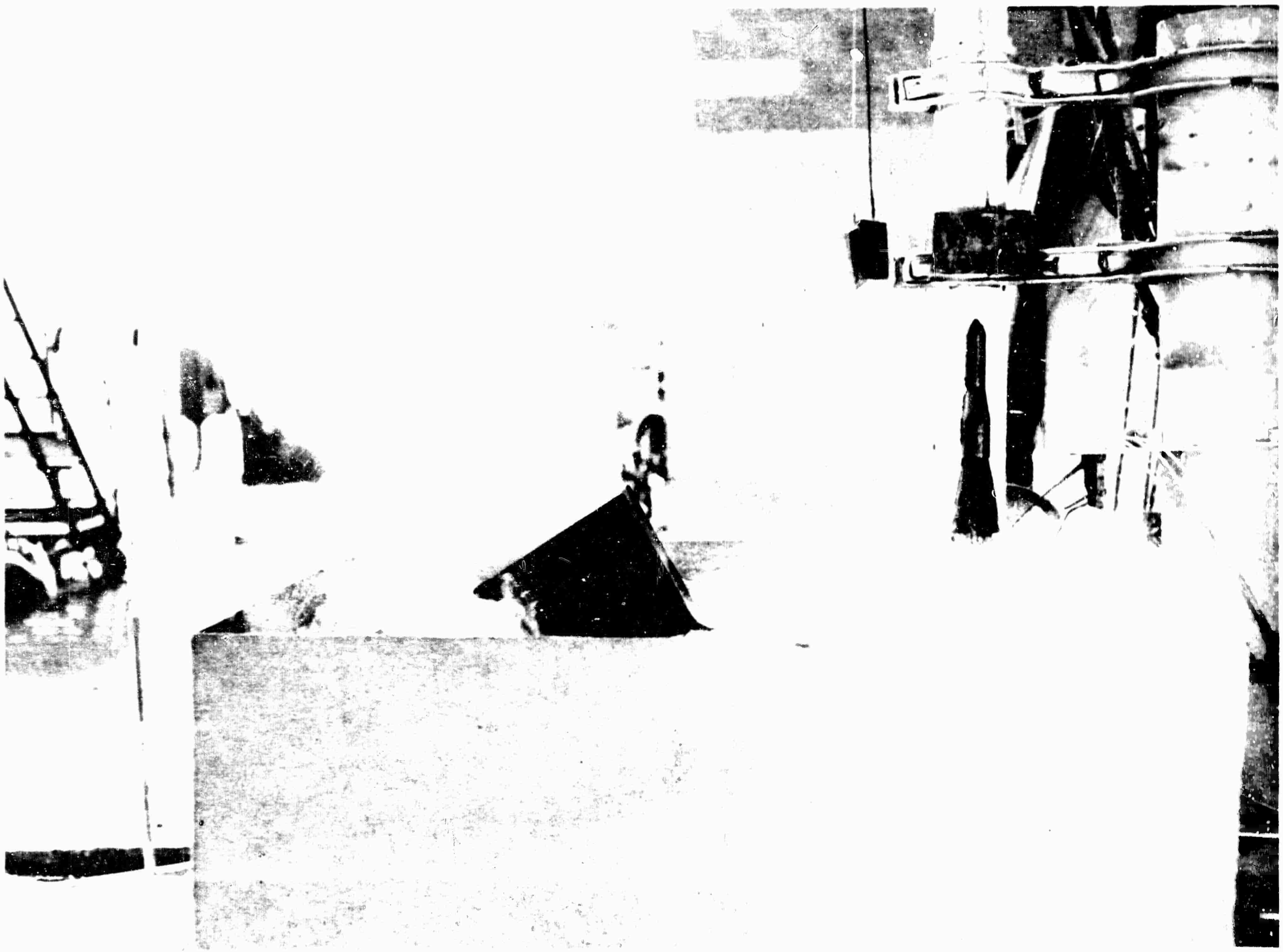

FIGURE 22 Flame Bucket Operation m=1/1
AE61-1140 Page 39

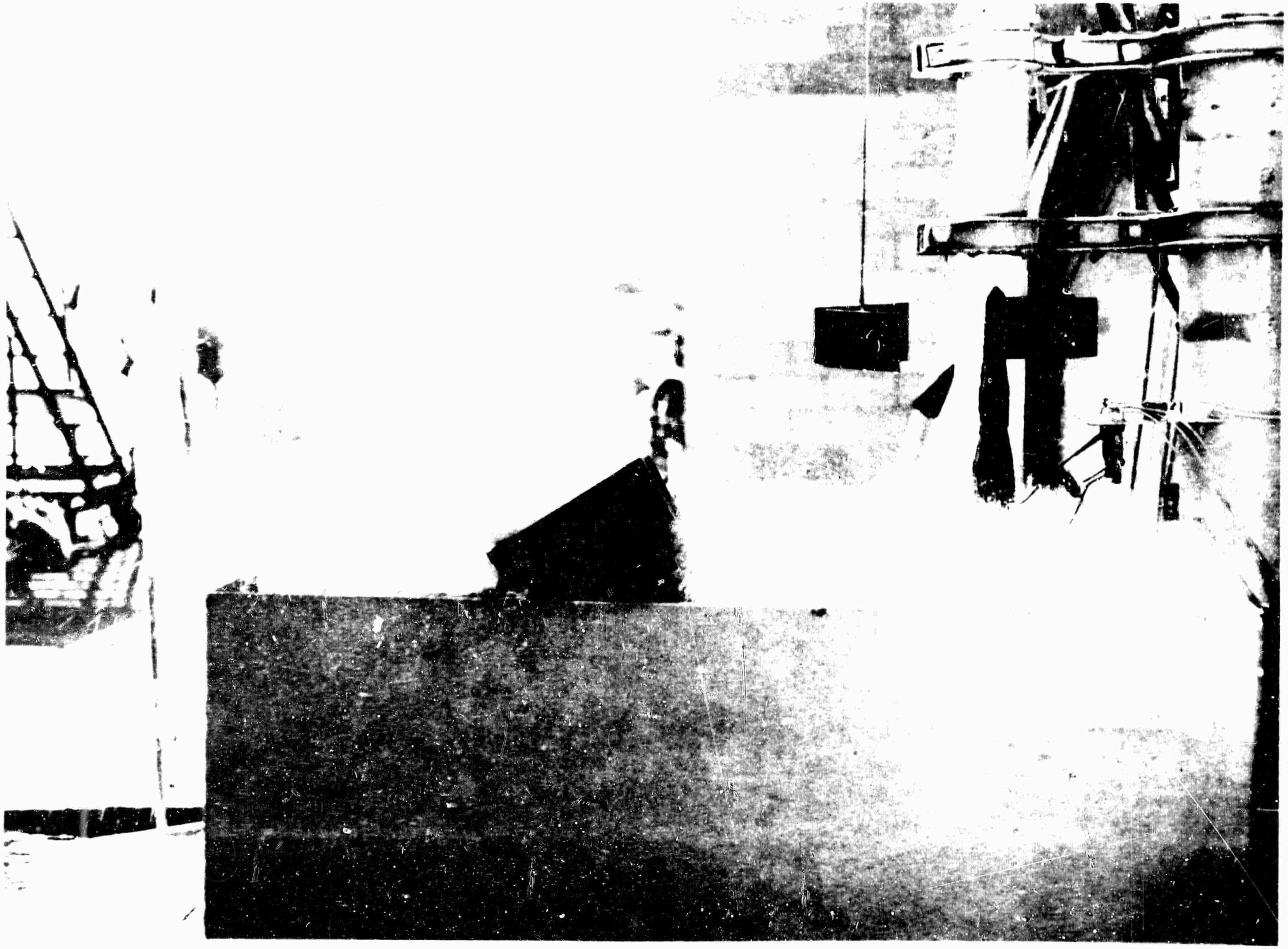

FIGURE 23 Flame Bucket Operation m=2/1
AE61-1140 Page 40

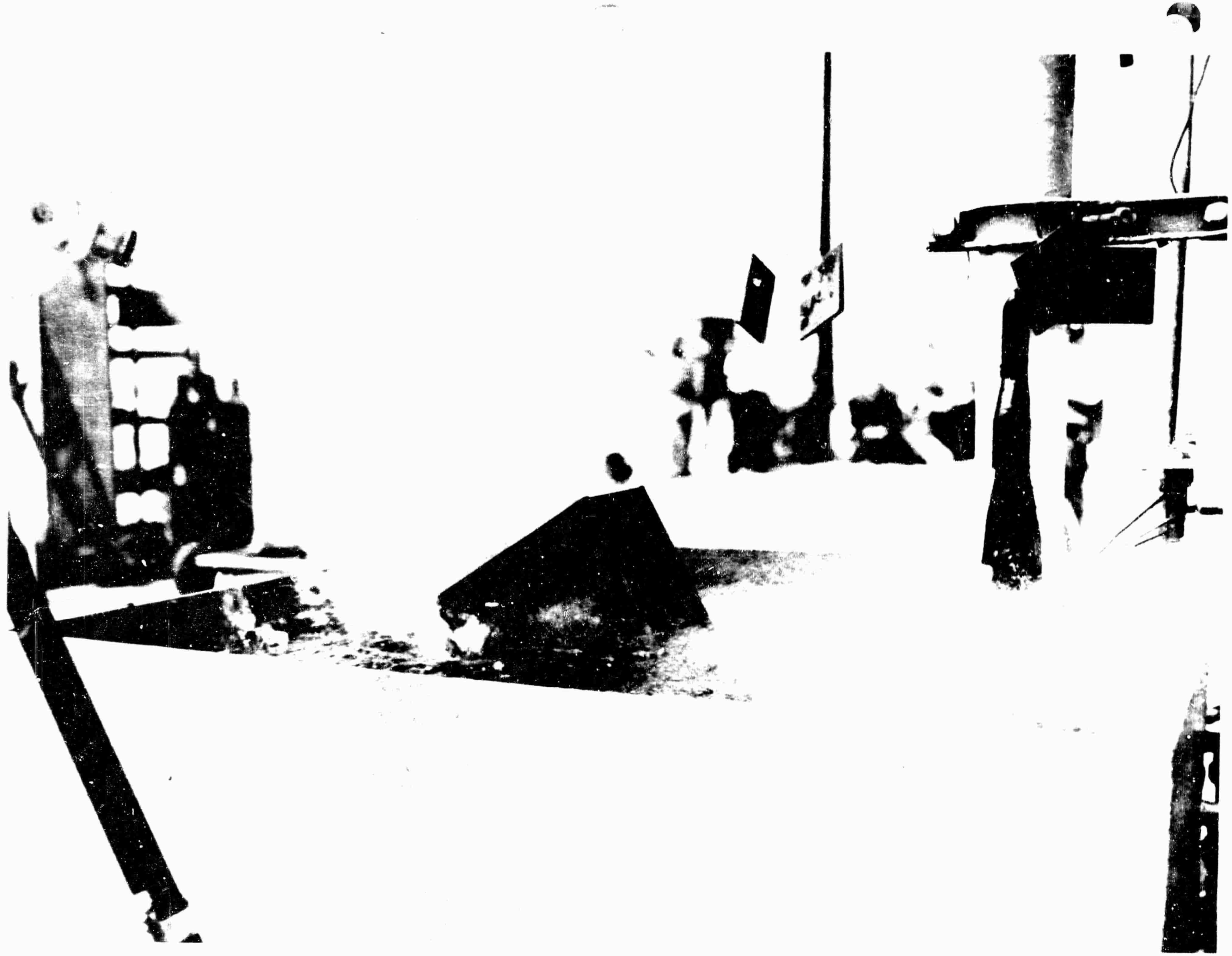

FIGURE 24 Flame Bucket Operation m=3/1

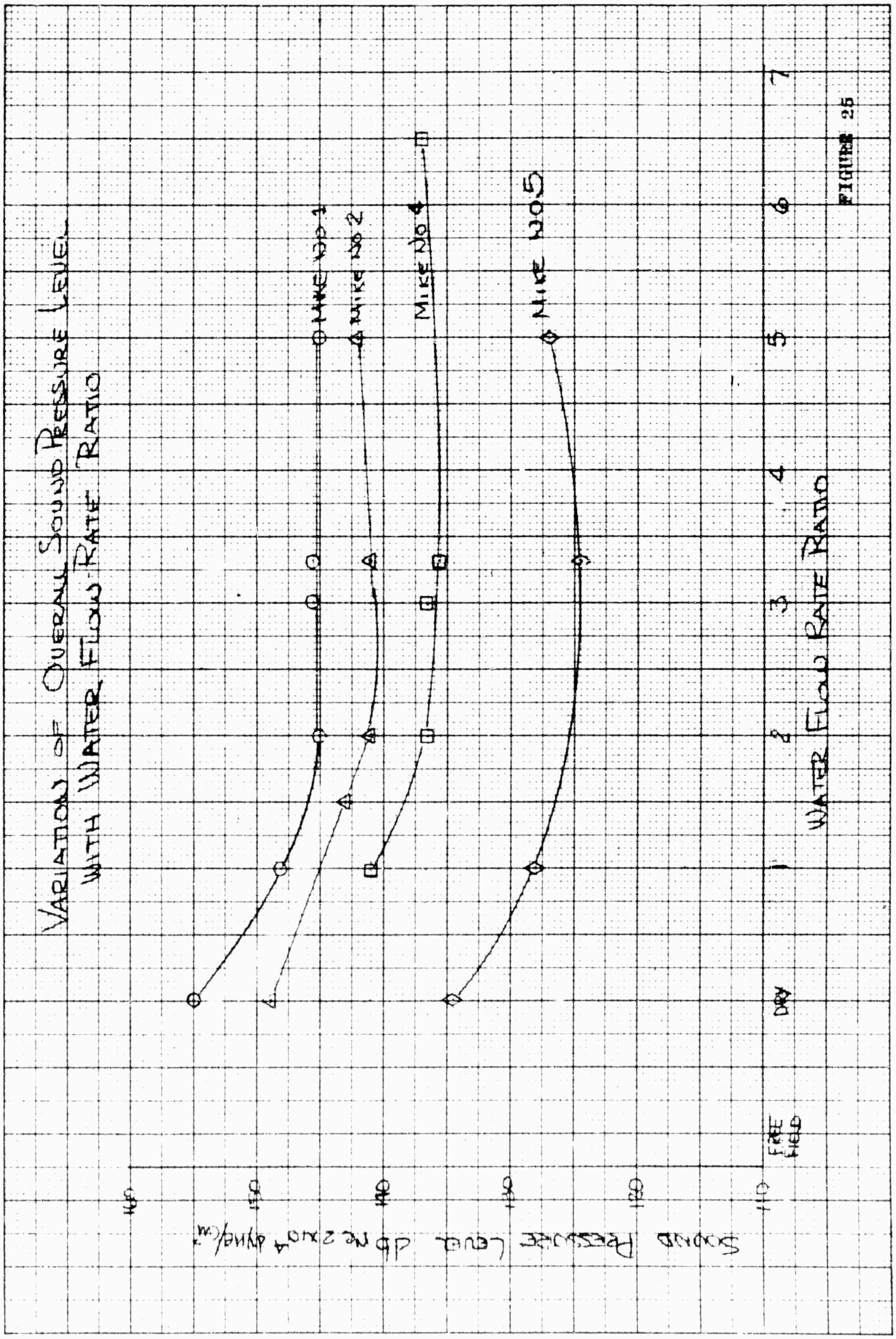
VARIATION OF OVERALL SOUND PRESSURE LEVEL
WITH WATER FLOW RATE RATIO
MIKE NO 1
MIKE NO 2
MIKE NO 4
MIKE NO 5
SOUND PRESSURE LEVEL db re 2x10^-4 dyne/cm^2
160
150
140
130
120
110
FREE FIELD
DRY
1
2
3
4
5
6
7
WATER FLOW RATE RATIO

FIGURE 25

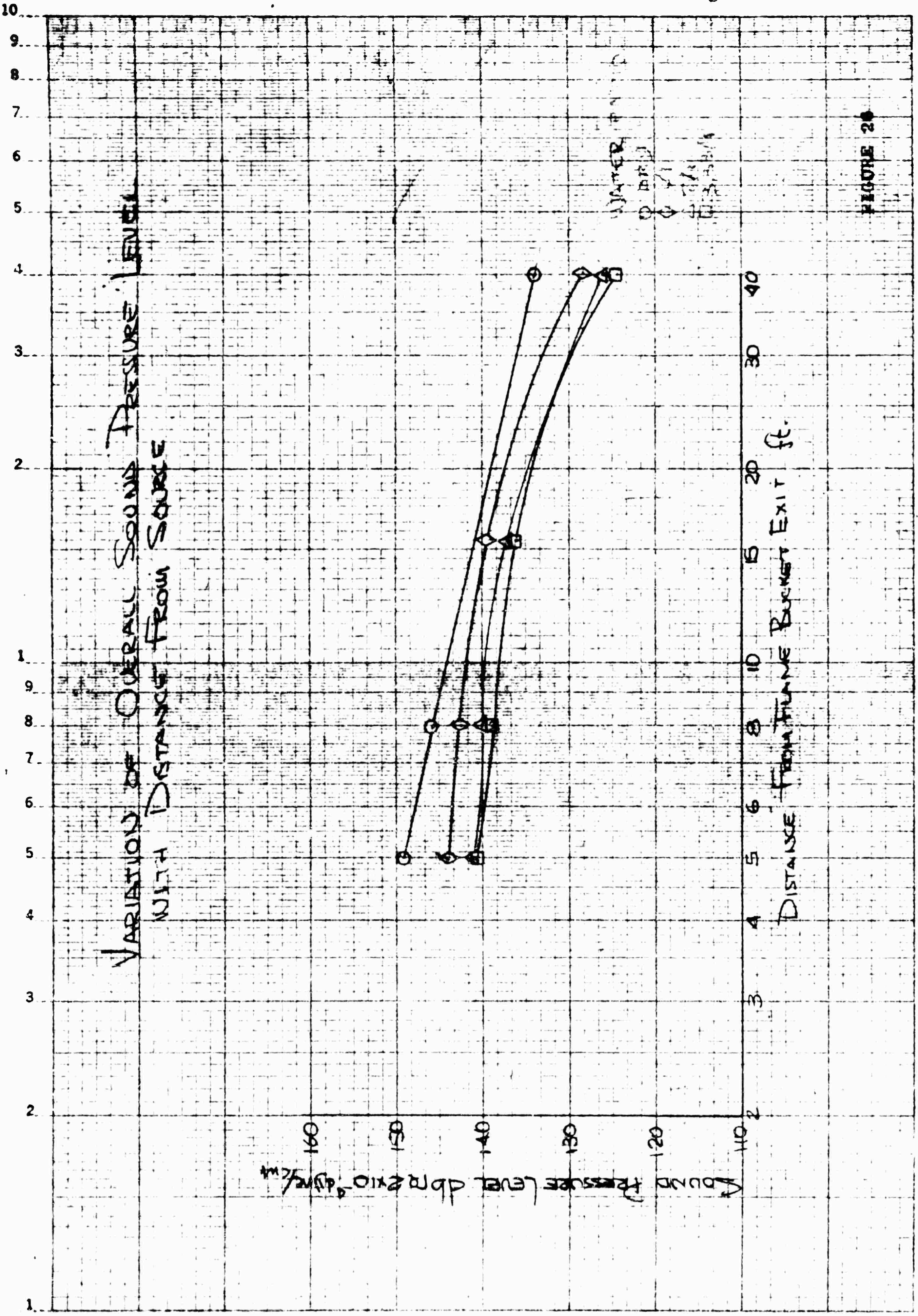
Variation of Overall Sound Pressure Level
With Distance From Source
Distance From Flame Bucket Exit ft.
Sound Pressure Level db re 2x10⁻⁴ dyne/cm²
160
150
140
130
120
110
2
3
4
5
6
8
10
15
20
30
40

FIGURE 26

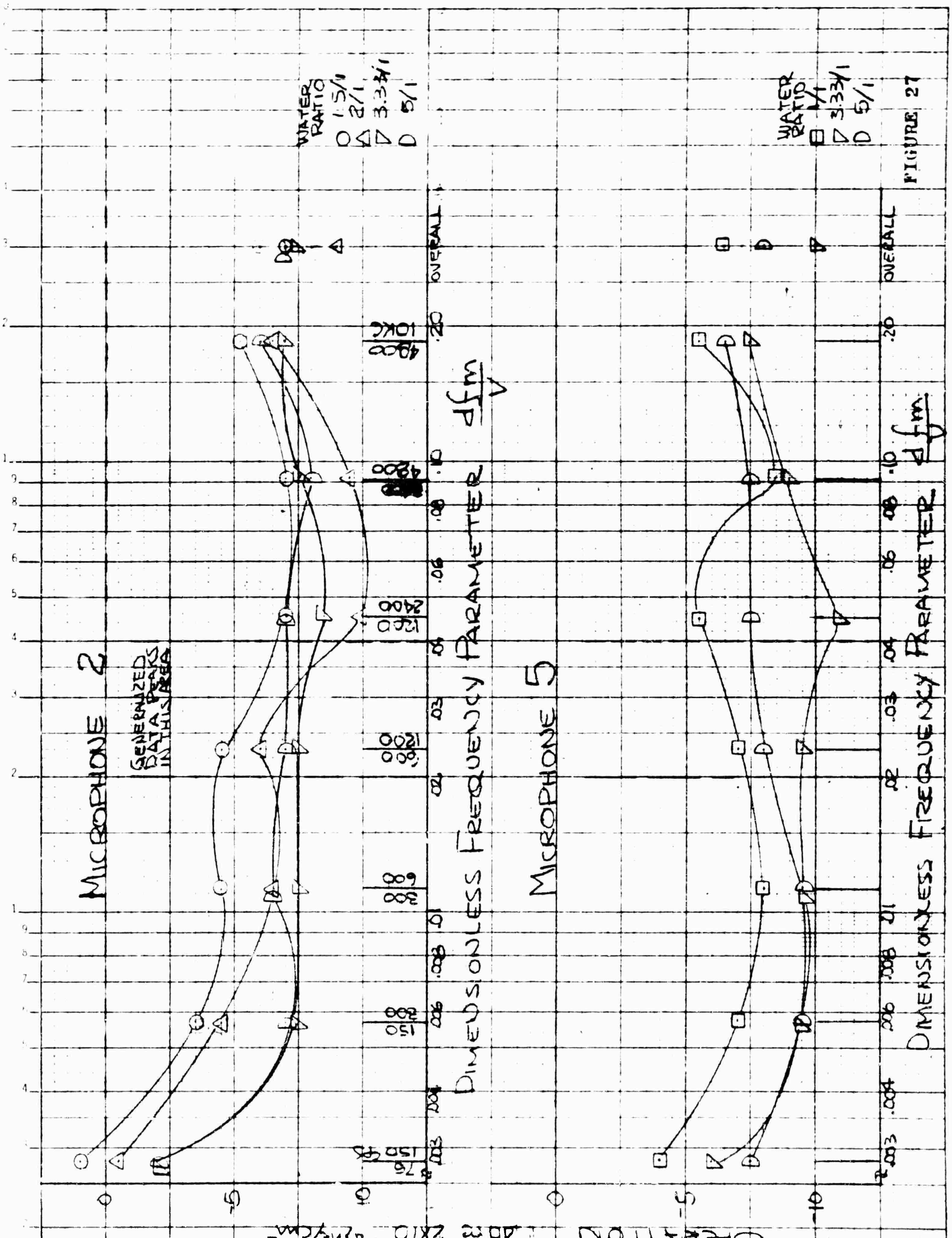
MICROPHONE 2
GENERALIZED DATA PEAKS IN THIS AREA
MICROPHONE 5
WATER RATIO
1.5/1
2/1
3.33/1
5/1
OVERALL
DIMENSIONLESS FREQUENCY PARAMETER d fm / V
SOUND PRESSURE LEVEL RELATIVE TO DRY OPERATION db re 2x10^-4 dyne/cm^2

FIGURE 27